Analysis of Conduction Band Offset Variation on the Electrostatics of UTB Devices through the Modified Effective Mass Approximation (mEMA)

SUBMISSION DATE / POSTED DATE

12-01-2022 / 18-01-2022

CITATION

Kansal, Harshit; Vilochan Mishra, Nalin; Solanki, Ravi; Medury, Aditya S (2022): Analysis of Conduction Band Offset Variation on the Electrostatics of UTB Devices through the Modified Effective Mass Approximation (mEMA). TechRxiv. Preprint. https://doi.org/10.36227/techrxiv.18262490.v1

DOI

10.36227/techrxiv.18262490.v1

Analysis of Conduction Band Offset Variation on the Electrostatics of UTB Devices through the Modified Effective Mass Approximation (mEMA)

Harshit Kansal,[1] Nalin Vilochan Mishra,[1] Ravi Solanki,[1] and Aditya Sankar Medury[1]
Department of Electrical Engineering and Computer Science
Indian Institute of Science Education and Research Bhopal, India

(*Electronic mail: harshit16@iiserb.ac.in)

(Dated: 18 December 2021)

In Ultra-thin Body (UTB) devices, besides the Ultra-thin (UT) nature of the channel, which manifests in terms of Quantum Confinement Effects (QCEs), the Band-offsets between the oxide and channel materials at their interface, also tends to strongly impact the channel electrostatics. Despite being very accurate in calculating the band-structure and hence considering QCEs for a given channel material, the Tight-Binding (TB) method tends to be more complicated to use at the channel/oxide interface of MOS devices, while on the other hand the Effective Mass Approximation (EMA) in spite of being less accurate, is a simpler approach to consider the effects of band-offsets at the interface. Given its accuracy, we firstly use the $sp^3d^5s^*$ TB method to calculate the Band-structure and then by considering significant k-points, efficiently incorporate the QCE into the electrostatics of Double-Gate (DG) Silicon-on-Insulator (SOI) MOS devices. Considering these results as a reference, with the assumption of an infinite potential well, we propose a modified Effective Mass Approximation (mEMA) approach, whereby introducing energy correction parameters, along with the effective mass parameters, all of which are shown to be gate bias, channel and oxide thickness dependent, the results obtained from the proposed approach are shown to have good agreement with the results from TB method. In order to analyze the effect of Conduction-Band Offset variations on the channel electrostatics parameters, we consider an SiO_2 layer of thickness of 1 *nm* and show the effect of different Band-offsets on the integrated charge density and gate capacitance, using the mEMA approach.

I. INTRODUCTION

In order to enable CMOS scaling, device structures such as fully-depleted, Ultra-Thin film silicon-on-insulator (UTSOI) MOSFETs have been considered due to their ability to significantly reduce short-channel effects[1,2], thus enabling their application in low-power digital[3] as well as Analog circuits[4]. With the scaling of the SOI channel and the oxide in UTB MOS structures, Quantum Confinement effects (QCEs)[5] along with carrier tunneling through Ultra-Thin oxides[6], together impact the channel electrostatics. Besides the Ultra-Thin oxide, the Band-offset at the oxide/channel interface becomes important to consider, as it impacts not just the carrier tunneling[7–9], but also the channel electrostatics parameters. While there has been considerable focus on quantifying the effect of band-offset variation on the tunneling current through the oxide[6], the effect of Band-offset variations at the oxide/channel interface, particularly for UTB MOSFETs, where QCEs tend to significantly manifest, needs to be more thoroughly understood in the context of channel electrostatics parameters such as the integrated charge density and the gate capacitance.

Quantum Confinement Effects seen in UTB MOS devices can be accurately taken into account by using the semi-empirical $sp^3d^5s^*$ Tight-Binding (TB) method, which generates the full-band structure[10]. By self-consistently solving the band-structure with the Poisson's equation, the electrostatics of the UTB DG SOI MOS devices can be simulated. However, the effect of considering a finite band offset at the channel/oxide interface, on the channel electrostatics, without first requiring the determination of the tunneling current is reported to be complicated and computationally cumbersome using the TB method[11,12]. Given that the effect of band-offset variations, has primarily been analyzed only in the context of direct tunneling current, a simplified and accurate approach is required to simulate the channel electrostatics, considering band-offset variations and QCEs, for UT MOS devices. In the context of full-band semi-empirical computational methods, it is useful to analyse the effective mass approximation (EMA)[13] as a possible approach, which has been successful in describing size and bias-induced quantization effects in Ultra-Thin channel devices[14].

While the results obtained from the EMA and the TB method are reported to match well for large SOI channel thicknesses, where QCEs are relatively less prevalent, however, for Ultra-thin (UT) channels, the results differ significantly due to the over-estimation of confinement energies in EMA Calculations[15]. The accurate estimation of channel electrostatics in the ultra-thin SOI channel requires: 1) consideration of structural confinement; and 2) consideration of the variation of band offset at the oxide-channel interface.

In order to accurately account for QCEs, in this work, we firstly modify the EMA approach, by introducing bias and thickness dependent energy correction terms for ground state and other excited states, along with effective mass parameters, while considering no wave function penetration inside the oxide (identical to high band offset). These energy correction terms and effective mass parameters are extracted through self-consistently bench-marking the electron carrier concentration and potential of the modified EMA (mEMA) approach with results obtained from the TB Method, over a wide range of SOI-channel thicknesses, oxide thickness and applied gate

biases. Having obtained the effective mass and energy correction parameters, for various channel and oxide thicknesses, we consider the case, where the thickness of the SiO_2 layer is 1 *nm*, for analyzing the effect of different band-offset values on the channel electrostatics parameters. By considering the thickness of the SiO_2 layer as being fixed (1 *nm*), we isolate the effect of insulator (barrier) thickness and instead analyze the effect of barrier height (band-offset) variations on the channel electrostatics parameters such as integrated charge density and gate capacitance.

The rest of the paper is organized as follows: In section II, the two simulation schemes considered in our work, for calculating the channel electrostatics of UTB devices, are briefly discussed, viz., the significant k-points based TB approach[16] and the effective mass approximation. In section III, we discuss the proposed modified effective mass approximation (mEMA) approach, outlining the various parameters, their importance and the procedure for their extraction through benchmarking with the results from the TB approach in the context of an infinite potential well. In section IV, we show the impact of considering Conduction-Band-Offset (CBO) variations on channel electrostatics parameters such as the channel charge density and gate capacitance, by using the proposed mEMA approach. Finally the conclusion is presented in section V.

II. SIMULATION SCHEME

Based on the well-known accuracy of the full-band structure approach, but with the use of the computationally efficient significant k-points based approach[16], a simplified yet accurate approach to simulate the channel electrostatics parameters, is discussed first. Next the EMA approach which serves as the basis for the proposed mEMA approach, is discussed.

A. Significant k-points based Approach

In order to efficiently and accurately simulate the channel electrostatics of UTB DG SOI MOSFETs, we use the significant k-points selection scheme, outlined by Solanki *et al.*[16]. Having selected the significant k-points, the band structure is solved self-consistently with the Poisson's equation, which is given as

$$\nabla^2\phi(z) = \frac{q\rho(z)}{\varepsilon} \tag{1}$$

where, ϕ is the electrostatic potential, ε is the channel's dielectric constant and $\rho(z)$ is the electron density along the direction of the channel thickness (T_{ch}). It may be noted that, the channel thickness is a function of the number of atomic layers (N), which, for the case of (100) surface, is given as $(N-1)\times a/4$. The boundary conditions at the top and bottom oxide-channel interface are the same as used by Majumdar *et al.*[17].

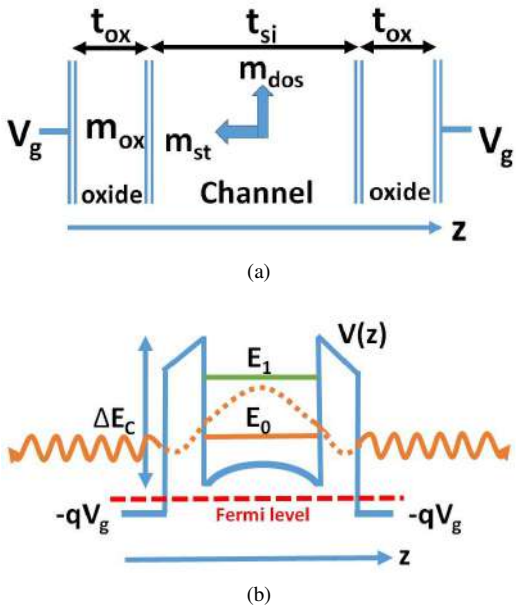

FIG. 1. (a) Effective mass parameters in the different regions of the device. (b) Conduction band diagram showing ground and first excited states inside the rectangular quantum well.

The electron density, $\rho(z)$, used in equation 1, is given below[18]:

$$\rho(z) = \sum_n \sum_k \frac{2g^k \Delta k_x \Delta k_y}{T_{ch}} \left(\frac{E_F - E_n^k}{kT}\right) |\psi_n^k(z)|^2 \Delta z \tag{2}$$

where, n is the number of energy levels in the conduction band, the factor F is the Fermi-Dirac probability, g^k is the degeneracy factor at each k-point, E_F is the Fermi level and $\psi_n^k(z)$ is the normalized wave-function along z direction. For an intrinsic channel the E_F will be equal to $E_g/2$.

Due to two possible spin states at each k-point, the factor of 2 is multiplied in the above equation. The double summation accounts for the contribution of various energy levels in the conduction band (n) at significant k points (E_n^k) in the BZ for electron density calculation. The potential energy ($-q\phi$) obtained by solving the Poisson's equation is added with the onsite energies at the diagonal of the TB Hamiltonian to consider the effect of potential on the band-structure. The resulting TB Hamiltonian is solved self-consistently with the Poisson's equation to obtain the channel charge density and potential at a given gate voltage (V_g).

B. Effective mass approximation (EMA) Methodology

We solve the Schrödinger equation inside the oxide and channel of UTB device, using the effective mass approximation. A single band of parabolic E-k relation is considered in both the channel as well as inside the oxide. The effective mass Schrödinger equation is given as:

$$-\frac{1}{2}\nabla.\left(\frac{1}{m^*(z)}\nabla\psi(z)\right) + V(z)\psi = E\psi(z) \tag{3}$$

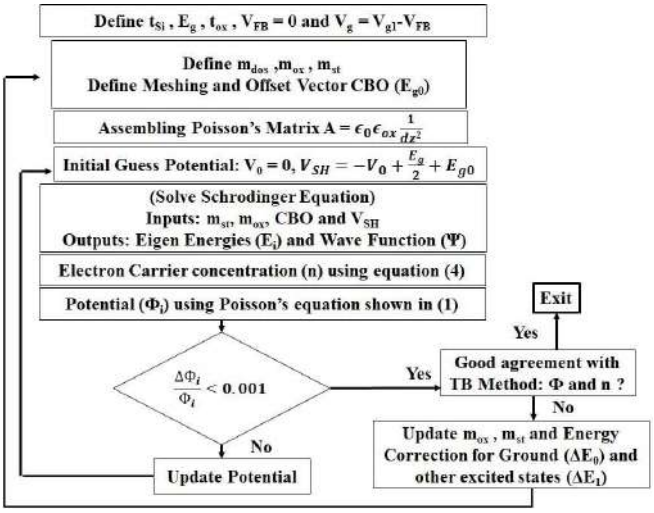

FIG. 2. Self-consistent procedure for extracting effective mass and energy correction parameters through determining electron carrier concentration and potential inside the SOI-channel, using the Effective Mass Parameters, bench-marked with electron carrier concentration and potential obtained from TB Method

where z is the tunneling direction, perpendicular to the oxide-channel interface. Along the direction of tunneling, m^* corresponds to m_{ox} (oxide tunneling mass) inside the oxide, while corresponding to m_{st} (semiconductor tunneling mass) inside the channel. All of these effective masses in the different regions are clearly shown in Figure 1 (a), V(z) is the potential energy profile in the z direction. The boundary condition for the voltage is defined at the metal-oxide interface, which is equal to the applied voltage at the gate terminal (V_g). The wave-function boundary condition is kept open at metal gate to consider leakage (tunneling) and to consider wave-function penetration in the oxide[19], as shown in Figure 1 (b). This penetration of wave-function depends on m_{ox} and ΔE_c (conduction band-offset between the SOI-channel and the oxide). The electron density inside the channel, using m_{dos} and wave-function (ψ), is calculated using[9]:

$$n(z) = \frac{k_B T}{\pi\hbar^2} g m_{dos} \sum_j \ln\left[1 + \exp\frac{(E_F - E_j)}{k_B T}\right] \psi_j^2(z) \qquad (4)$$

where g and m_{dos} are the valley degeneracy ($g = 1$ for Γ valley) and the density-of-states effective mass, respectively, while ψ_j is the wave function for the j^{th} sub-band. ψ_j and E_j in equation (4) are obtained from solving the one-dimensional effective mass Schrödinger equation. In equation (4), for calculating the electron carrier concentration, we consider the contribution of the ground and first excited states. The effective mass Schrödinger equation is solved self-consistently with the Poisson's equation, using numerical techniques (Finite element method and Newton-Raphson method), where, a suitable choice of the effective mass parameters enables the EMA approach to be more accurate for thicker SOI channels, where QCEs are not very significant.

III. MODIFIED EFFECTIVE MASS APPROXIMATION

The inability of the EMA approach to accurately account for QCEs, in ultra-scaled devices, for $t_{Si} \leq 5$ nm, requires modification to the existing EMA approach, where by introducing bias (gate voltage) and thickness dependent (t_{Si} and t_{ox}) energy correction and effective mass parameters to the existing EMA approach, we are now able to match the electron carrier concentration and potential obtained from the mEMA approach with the TB method. There are five parameters in the proposed mEMA approach which includes:

ΔE_0: energy correction term to the ground state of the conduction band, which enables this approach to account for structural confinement effects.

ΔE_1: common energy correction to the first and higher excited states of the conduction band, which enables the consideration of charge confinement effects.

m_{dos}: Density-of-states effective mass which is extracted form the band-structure, obtained form the TB method, around the band minima of the Γ valley, found to be channel thickness and bias independent, with a value of $0.23\ m_0$.

m_{st}: semiconductor tunneling mass which is channel thickness and bias dependent.

m_{ox}: oxide tunneling mass which varies with oxide thickness (t_{ox}) and is independent of both channel thickness and the applied bias.

Utilizing the methodology outlined in Figure 2, the electron carrier concentration is determined based on equation 4. Having obtained the electron carrier concentration, the potential is calculated using the Poisson's equation by using a self-consistent procedure shown in Figure 2. From equation (4), it may be noted that it becomes possible for the mEMA approach to more accurately account for structural confinement effects, through the introduction of energy correction terms, for a wide range of channel thicknesses, shown for $t_{Si} = 2$ nm and $t_{Si} = 10$ nm, in Figure 3. In Figure 3, the corrected energies from the mEMA approach are compared with the energies obtained from the EMA approach (energies uncorrected, but with the same effective masses as the mEMA approach). It may be seen from Figure 3, that for $t_{Si} = 2$ nm, where structural confinement effects are significant, the corrected ground state of the mEMA (with energy correction) is higher than the ground state of the EMA, for almost the entire range of gate voltages, while on the other hand, for $t_{Si} = 10$ nm, the corrected energy terms are significantly higher at lower gate voltages. Also, from Figure 3, for the higher gate voltages, it is seen that the ground state and first excited state of the mEMA and EMA approaches are shown to be much closer. Besides, the energy correction terms, another important and distinct aspect of the proposed mEMA approach is the bias (gate voltage), channel thickness dependence of m_{st} and oxide thickness dependence of m_{ox}, which enables good agreement with the simulation results from the TB method. The values of these effective mass parameters and energy correction terms are shown in the supplementary material (for Si channel and SiO_2 oxide layer). Through these effective mass and energy correction parameters, the electron density and the electrostatic potential along the SOI-channel thickness obtained

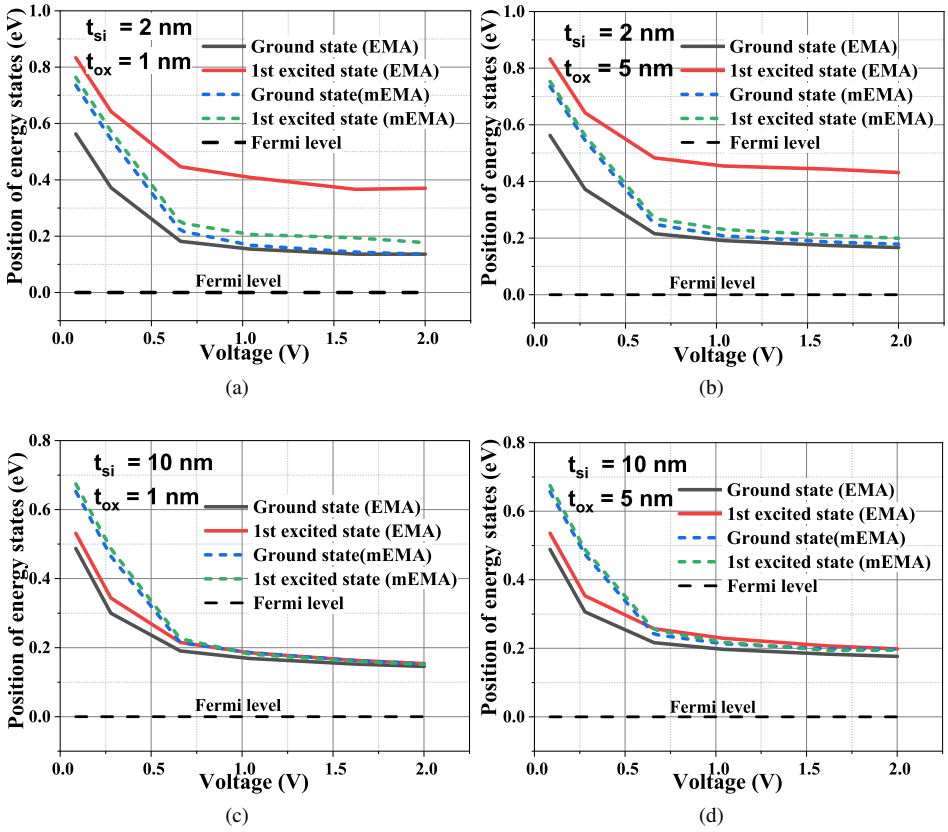

FIG. 3. Position of energy states (ground-state and 1st excited state) in EMA and mEMA approach for (a) $t_{Si} = 2\ nm$, $t_{ox} = 1\ nm$; (b) $t_{Si} = 2\ nm$, $t_{ox} = 5\ nm$; (c) $t_{Si} = 10\ nm$, $t_{ox} = 1\ nm$; and (d) $t_{Si} = 10\ nm$, $t_{ox} = 5\ nm$

through the mEMA approach is compared with results from the TB method, in Figures 4 and 5, respectively, for channel thicknesses (t_{Si}) of 2 *nm* and 10 *nm* and oxide thickness (t_{ox}) of 1 *nm* and 5 *nm*, for different gate voltages, where good agreement may be seen, which confirms the validity of extracted parameters. Also, a good match of integrated charge density can be seen, over the entire range of gate voltages considered (see supplement). It is important to clearly point out that in this process of bench-marking the mEMA approach with the TB method, the effect of tunneling is neglected (for an infinite potential well), by considering the Conduction band offset between the thin silicon channel and the oxide to be very high (8.15 eV).

IV. EFFECT OF BAND-OFFSET VARIATIONS ON CHANNEL ELECTROSTATICS PARAMETERS

The Band-offset at the oxide/channel interface can be interpreted as a reduction in the height of the potential well, thereby impacting the channel electrostatics parameters, such as the electron carrier concentration, integrated charge density and gate capacitance. In UTB DG SOI MOS devices, given the strong prevalence of QCEs, particularly for $t_{Si} < 5$ *nm*, the impact of band-offset variations either on enhancing or mitigating QCEs, needs to be clearly analyzed, in terms of these channel electrostatics parameters. In this section, in order to analyze the impact of band-offset variations, at the channel/oxide interface, we consider the SiO_2 layer to have a fixed physical thickness of 1 *nm*. This enables us to clearly analyze the effect of CBO variations on channel electrostatics parameters. In the mEMA approach, the CBOs are included as an input, which changes the barrier height and hence the potential energy and can be used to calculate the various electrostatics parameters, by using the procedure outlined in Figure 2. It is important to point out that the extracted energy correction parameter and effective mass parameters for various channel thicknesses and oxide thicknesses are independent of CBO variation at the interface.

By considering CBOs ranging from 8.15 eV (infinite potential well) to 0.8 eV (approximately similar to CBO of Gd_2O_3 with Silicon), we show the effect of CBO variations on the electron carrier concentration for different gate voltages and SOI channel thicknesses. The effect of band-offset reduction impacts the electron concentration differently, for $t_{Si} = 2\ nm$ compared to $t_{Si} = 10\ nm$, and is discussed in detail below:

- Due to strong structural confinement effects, for $t_{Si} = 2$ *nm*, where the band-gap is much higher than its bulk value, implying that all states of the conduction band are located at higher energy values. This means that most conduction electrons are located in the ground-

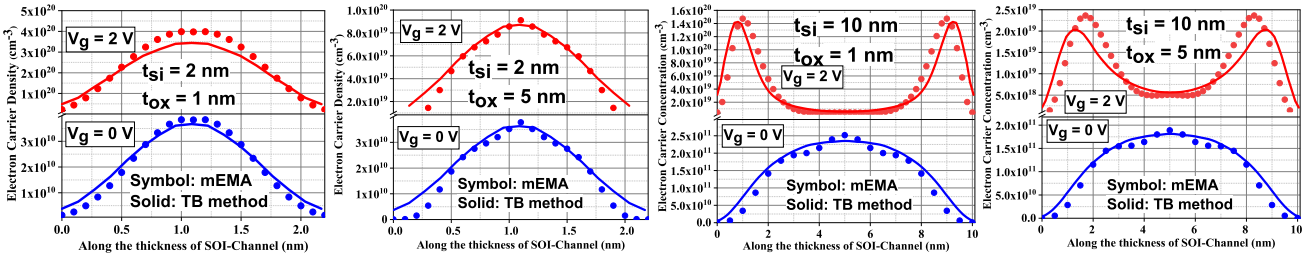

(a) $m_{ox} = 0.9m_0$, $m_{st} = 0.76m_0$ ($V_g = 0V$), $m_{st} = 0.72m_0$ ($V_g = 2V$)

(b) $m_{ox} = 0.4m_0$, $m_{st} = 0.74m_0$ ($V_g = 0V$), $m_{st} = 0.7m_0$ ($V_g = 2V$)

(c) $m_{ox} = 0.9m_0$, $m_{st} = 0.23m_0$ ($V_g = 0V$), $m_{st} = 0.18m_0$ ($V_g = 2V$)

(d) $m_{ox} = 0.4m_0$, $m_{st} = 0.21m_0$ ($V_g = 0V$), $m_{st} = 0.18m_0$ ($V_g = 2V$)

FIG. 4. Electron Carrier Concentration along the depth of the SOI-Channel; $m_{dos} = 0.23m_0$, showing good agreement between mEMA and TB Method for (a) $t_{Si} = 2nm$, $t_{ox} = 1nm$ (b) $t_{Si} = 2nm$, $t_{ox} = 5nm$ (c) $t_{Si} = 10nm$, $t_{ox} = 1nm$ (d) $t_{Si} = 10nm$, $t_{ox} = 5nm$

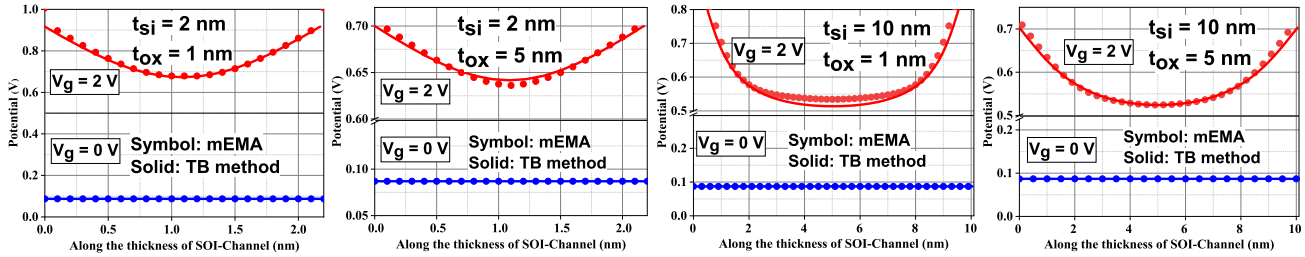

(a) $m_{ox} = 0.9m_0$, $m_{st} = 0.76m_0$ ($V_g = 0V$), $m_{st} = 0.72m_0$ ($V_g = 2V$)

(b) $m_{ox} = 0.4m_0$, $m_{st} = 0.74m_0$ ($V_g = 0V$), $m_{st} = 0.7m_0$ ($V_g = 2V$)

(c) $m_{ox} = 0.9m_0$, $m_{st} = 0.23m_0$ ($V_g = 0V$), $m_{st} = 0.18m_0$ ($V_g = 2V$)

(d) $m_{ox} = 0.4m_0$, $m_{st} = 0.21m_0$ ($V_g = 0V$), $m_{st} = 0.18m_0$ ($V_g = 2V$)

FIG. 5. Electrostatic Potential along the depth of the SOI-Channel; $m_{dos} = 0.23m_0$, showing good agreement between mEMA and TB Method for (a) $t_{Si} = 2nm$, $t_{ox} = 1nm$ (b) $t_{Si} = 2nm$, $t_{ox} = 5nm$ (c) $t_{Si} = 10nm$, $t_{ox} = 1nm$ (d) $t_{Si} = 10nm$, $t_{ox} = 5nm$

state (E_0), thus resulting in the higher excited states being largely vacant. This also implies that the relative band-offsets at the interface, between the oxide and the conduction band of the UT channel is reduced due to strong structural confinement effects. Amongst the states of the conduction band, probabilistically most electrons that tunnel through the oxide, occupy the first excited state, which is mostly vacant and has a much reduced band-offset compared to the ground state. This manifests in terms of a symmetric twin peak in the electron concentration profile, with reducing band-offsets, over a wide range of gate voltages, as shown in Figures 6 (a) and 6 (b).

- On the other hand, for $t_{Si} = 10\,nm$, where structural confinement effects have significantly receded, the band-gap is relatively closer to the bulk band-gap. Also, the various states of the conduction band are located at lower energy values (closer to semi-classical values), which are relatively closer to each other, resulting in higher CBO compared to $t_{Si} = 2\,nm$. Therefore, with the decrease in the CBO between the oxide and the channel, for $t_{Si} = 10\,nm$, fewer electrons tunnel through the oxide and occupy the first excited state, as shown in Figures 6 (c) and 6 (d). Also, it is important to note that, for $t_{Si} = 10\,nm$, even in the infinite potential well, the population of the first excited state is non-negligible, even for lower gate voltages. This first excited state population is further increased due to band-offset reduction, particularly at higher gate voltages, where the tunneling through the oxide, results in higher electron concentration (twin peak behavior) closer to the top/bottom surface.

- The relatively large effect of band-offset reduction, for $t_{Si} = 2\,nm$ compared to $t_{Si} = 10\,nm$, manifests in terms of a far more significant impact on the integrated charge density, over a wide range of gate voltages, as shown in Figure 7. On the other-hand, for $t_{Si} = 10\,nm$, the effect of band-offset reduction is negligible for lower gate voltages and only marginally impacts the integrated charge density at higher gate voltages.(see linear scale plot in Figure 7 (b))

- The decrease in ground-state electron population, with decrease in CBOs, particularly for $t_{Si} = 2\,nm$, indicates a reduction in the field-effect and therefore, the gate capacitance, with increase in direct tunneling through the oxide, which is shown in Figure 8 (a). This field effect degradation is particularly apparent for higher gate voltages. In order to enable the determination of the gate capacitance, we neglect the effect of tunneling through the oxide, by considering the contribution of the first and higher excited states to be the same as the infinite

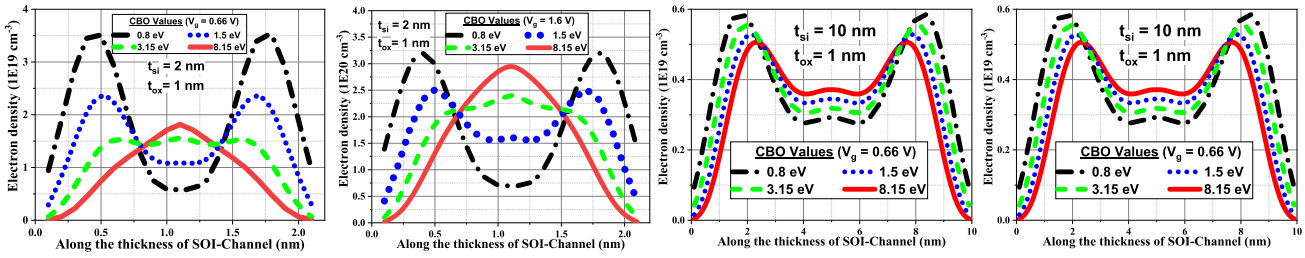

FIG. 6. Electron carrier concentration along the depth with different CBOs for (a) $t_{Si} = 2\ nm$ at V_g = 0.66 V (b) $t_{Si} = 2\ nm$ at V_g = 1.6 V (c) $t_{Si} = 10\ nm$ at V_g = 0.66 V and (d) $t_{Si} = 10\ nm$ at V_g = 1.6 V.

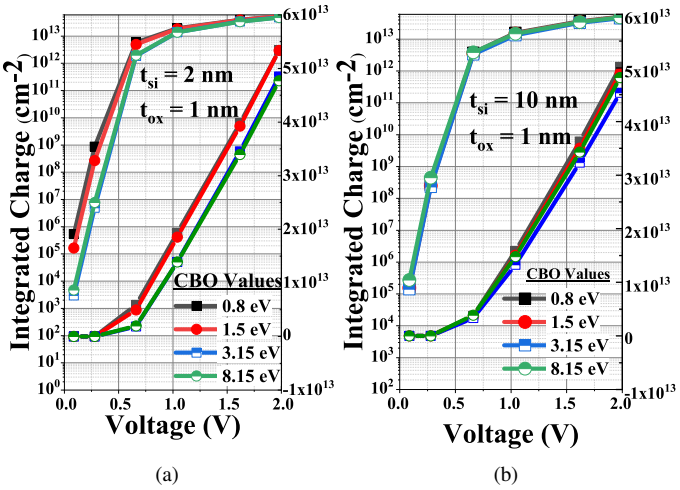

FIG. 7. Integrated Charge (Linear and Log scale) versus gate voltage with $t_{ox} = 5\ nm$ for (a) $t_{Si} = 2\ nm$ and (b) $t_{Si} = 10\ nm$, showing effect of CBO variation.

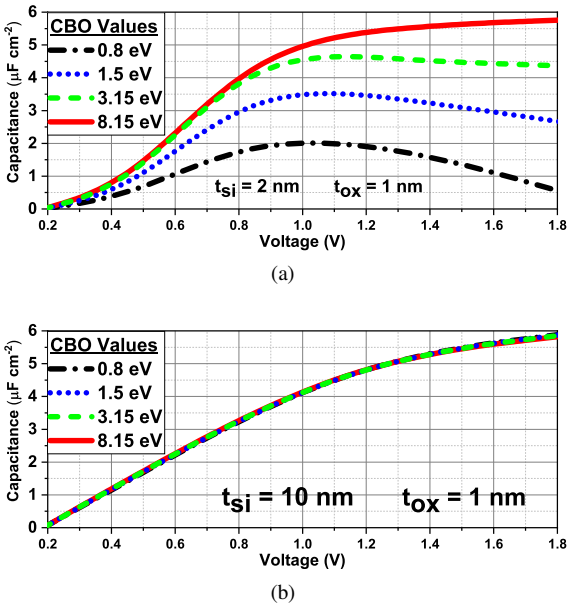

FIG. 8. Gate Capacitance versus Voltage at different CBOs for (a) $t_{Si} = 2\ nm$, $t_{ox} = 1\ nm$; and (b) $t_{Si} = 10\ nm$, $t_{ox} = 1\ nm$, while neglecting the increase in higher excited state population due to carrier tunneling through the oxide.

potential well, regardless of band-offset variations. This basically means that we consider the effect of Band-offset reduction only on the ground-state population, where the ground-state electron population is shown to decrease with decreasing Band-offsets. This manifests in terms of a lower integrated charge density and thus a lower gate capacitance, with reducing CBOs, for $t_{Si} = 2$ *nm* (see Figure 7 (a) and Figure 8 (a)). Also, at higher gate voltages, for $t_{Si} = 2\ nm$, it is seen that with greater electron charge tunneling through the oxides with reducing CBOs, the gate capacitance decreases implying much diminished Field-effect (gate control). On the other-hand for $t_{Si} = 10\ nm$, the effect of CBO reduction is far lower, having negligible impact on the ground-state population and thus on the integrated charge and gate capacitance (see Figure 7 (b) and Figure 8 (b)). This basically means that, for the case of $t_{Si} = 10\ nm$, since QCEs are far less significant, hence effect of CBO reduction on the channel electrostatics, is relatively less for $t_{Si} = 10\ nm$ case compared to $t_{Si} = 2\ nm$ case.

Through this comprehensive analysis, we have separated the effect of band-offset variations on the channel electrostatics, by quantifying the impact of these variations on carrier tunneling through the oxide in terms of the electron concentration as well as determining the degradation in the gate capacitance due to band-offset reduction. This has enabled us to show that, for $t_{Si} = 2\ nm$, where structural confinement effects are predominant, the effects of carrier tunneling through the oxide and the degradation of the gate capacitance are both more significant, than at $t_{Si} = 10\ nm$.

V. CONCLUSION

In this work, through the introduction of energy correction parameters for the ground-state and other higher excited states, and through the consideration of gate bias, channel thickness and oxide thickness dependence of the energy cor-

rection and effective mass parameters, a modified EMA approach (mEMA) was proposed and shown to agree well with the results from the TB approach, for an infinite potential well. This then enabled, a simplified analysis of the effect of conduction band-offset variations on various electrostatics parameters such as electron carrier concentration, integrated charge and gate capacitance, clearly demonstrating diminished field-effect coinciding with higher tunneling of electron charge through the oxide, for those channel thicknesses where Quantum Confinement Effects are significant.

SUPPLEMENTARY MATERIAL

The values for extracted Effective Mass parameters along with energy correction terms for ground and other excited states over a wide range of voltages, considering no tunneling of carriers through the oxide, for SOI-channel thicknesses $t_{Si} = 2$ *nm* to $t_{Si} = 10$ *nm* with oxide thicknesses of $t_{ox} = 1$ *nm* and $t_{ox} = 5$ *nm*, ensuring excellent agreement with Tight-Binding (TB) Method, in terms of electron carrier concentration and potential, is given in the supplementary material.

ACKNOWLEDGEMENT

We acknowledge financial support from CSIR, Government of India (Grant No: CSIR/EEC/2019027).

REFERENCES

[1] Y.-K. Choi, K. Asano, N. Lindert, V. Subramanian, T.-J. King, J. Bokor, and C. Hu, "Ultra-thin body soi mosfet for deep-sub-tenth micron era," in *International Electron Devices Meeting 1999. Technical Digest (Cat. No. 99CH36318)* (IEEE, 1999) pp. 919–921.

[2] E. Suzuki, K. Ishii, S. Kanemaru, T. Maeda, T. Tsutsumi, T. Sekigawa, K. Nagai, and H. Hiroshima, "Highly suppressed short-channel effects in ultrathin soi n-mosfets," IEEE Transactions on Electron Devices **47**, 354–359 (2000).

[3] S. Monfray, C. Fenouillet-Beranger, G. Bidal, F. Boeuf, S. Denorme, J. Huguenin, M. Samson, N. Loubet, J. Hartmann, Y. Campidelli, *et al.*, "Thin-film devices for low power applications," Solid-state electronics **54**, 90–96 (2010).

[4] V. Kilchytska, M. M. Arshad, S. Makovejev, S. Olsen, F. Andrieu, T. Poiroux, O. Faynot, J.-P. Raskin, and D. Flandre, "Ultra-thin body and thin-box soi cmos technology analog figures of merit," Solid-State Electronics **70**, 50–58 (2012).

[5] X. Guan and Z. Yu, "Atomistic approach to thickness-dependent bandstructure calculation of insb utb," IEEE transactions on nanotechnology **6**, 101–105 (2007).

[6] S.-H. Lo, D. Buchanan, Y. Taur, and W. Wang, "Quantum-mechanical modeling of electron tunneling current from the inversion layer of ultra-thin-oxide nmosfet's," IEEE Electron Device Letters **18**, 209–211 (1997).

[7] J. C. Ranuárez, M. J. Deen, and C.-H. Chen, "A review of gate tunneling current in mos devices," Microelectronics reliability **46**, 1939–1956 (2006).

[8] G. Darbandy, R. Ritzenthaler, F. Lime, I. Garduño, M. Estrada, A. Cerdeira, and B. Iñiguez, "Analytical modeling of the gate tunneling leakage for the determination of adequate high-k dielectrics in double-gate soi mosfets at the 22 nm node," Solid-State Electronics **54**, 1083–1087 (2010).

[9] S.-H. Lo, D. A. Buchanan, and Y. Taur, "Modeling and characterization of quantization, polysilicon depletion, and direct tunneling effects in mosfets with ultrathin oxides," IBM Journal of Research and Development **43**, 327–337 (1999).

[10] Y. Liu, N. Neophytou, G. Klimeck, and M. S. Lundstrom, "Band-structure effects on the performance of iii–v ultrathin-body soi mosfets," IEEE Transactions on Electron Devices **55**, 1116–1122 (2008).

[11] Y. Hou, M. Li, Y. Jin, and W. Lai, "Direct tunneling hole currents through ultrathin gate oxides in metal-oxide-semiconductor devices," Journal of applied physics **91**, 258–264 (2002).

[12] M. Städele, B. Tuttle, K. Hess, and L. Register, "Tight-binding investigation of electron tunneling through ultrathin sio2gate oxides," Superlattices and Microstructures **27**, 405–409 (2000).

[13] Z. M. Gibbs, F. Ricci, G. Li, H. Zhu, K. Persson, G. Ceder, G. Hautier, A. Jain, and G. J. Snyder, "Effective mass and fermi surface complexity factor from ab initio band structure calculations," npj Computational Materials **3**, 1–7 (2017).

[14] Y. Hou and M.-F. Li, "Hole quantization effects and threshold voltage shift in pmosfet-assessed by improved one-band effective mass approximation," IEEE Transactions on Electron Devices **48**, 1188–1193 (2001).

[15] Y. Niquet, C. Delerue, G. Allan, and M. Lannoo, "Method for tight-binding parametrization: Application to silicon nanostructures," Physical Review B **62**, 5109 (2000).

[16] R. Solanki, N. V. Mishra, and A. S. Medury, "Significant k-point selection scheme for computationally efficient band structure based utb device simulations," Semiconductor Science and Technology **36**, 115009 (2021).

[17] K. Majumdar and N. Bhat, "Bandstructure effects in ultra-thin-body double-gate field effect transistor: A fullband analysis," Journal of Applied Physics **103**, 114503 (2008).

[18] A. Rahman, G. Klimeck, T. B. Boykin, and M. Lundstrom, "Bandstructure effects in ballistic nanoscale mosfets," in *IEDM Technical Digest. IEEE International Electron Devices Meeting, 2004.* (IEEE, 2004) pp. 139–142.

[19] R. Ram-Mohan and L. R. Ram-Mohan, *Finite element and boundary element applications in quantum mechanics*, Vol. 5 (Oxford University Press on Demand, 2002).

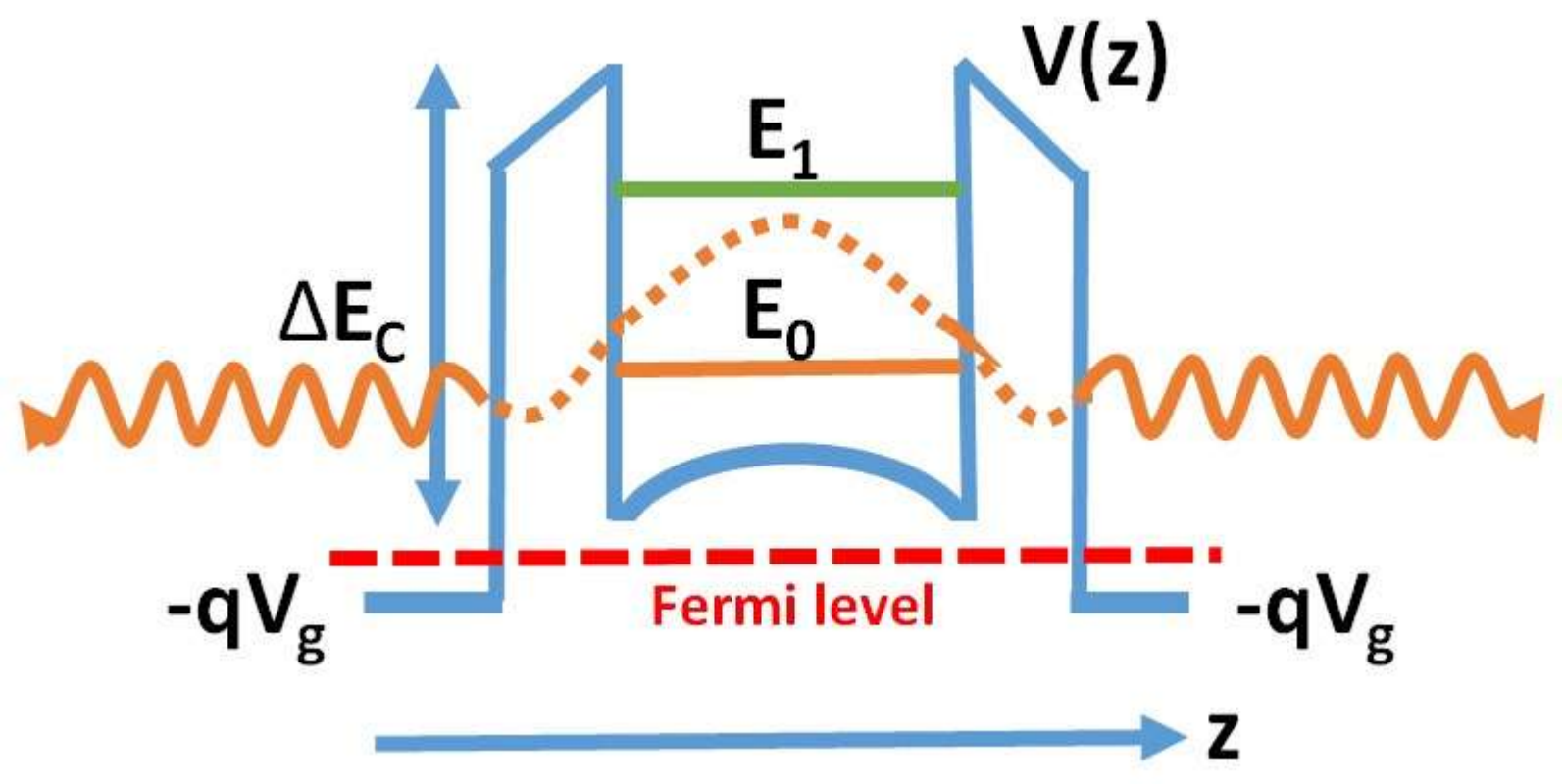
V(z)
E1
E0
ΔEC
-qVg
Fermi level
-qVg
z

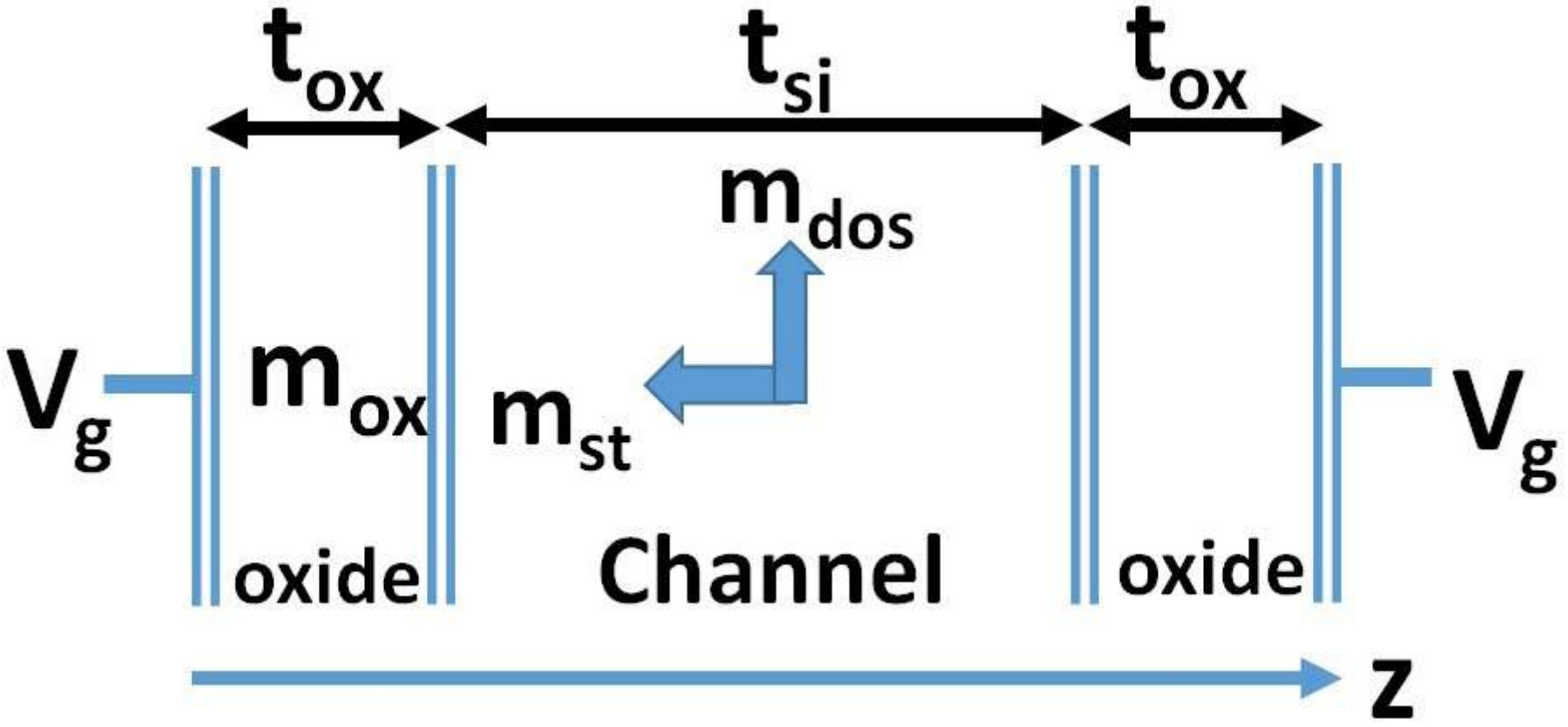
t_{ox}
t_{si}
t_{ox}
m_{dos}
V_g
m_{ox}
m_{st}
V_g
oxide
Channel
oxide
z

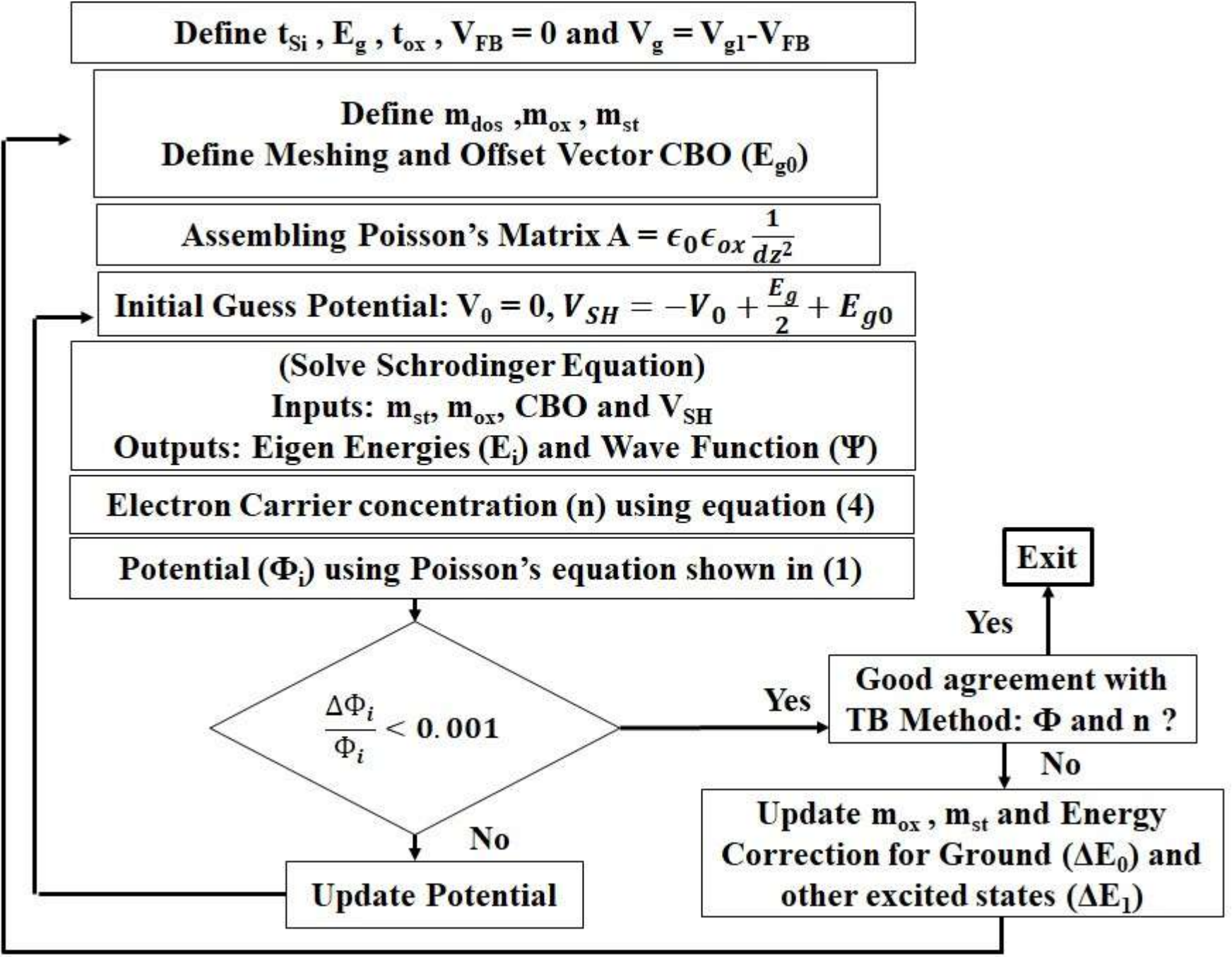
Define t_{Si} , E_g , t_{ox} , $V_{FB} = 0$ and $V_g = V_{g1}-V_{FB}$
Define m_{dos} ,m_{ox} , m_{st}
Define Meshing and Offset Vector CBO (E_{g0})
Assembling Poisson's Matrix A = $\epsilon_0 \epsilon_{ox} \frac{1}{dz^2}$
Initial Guess Potential: $V_0 = 0$, $V_{SH} = -V_0 + \frac{E_g}{2} + E_{g0}$
(Solve Schrodinger Equation)
Inputs: m_{st}, m_{ox}, CBO and V_{SH}
Outputs: Eigen Energies (E_i) and Wave Function (Ψ)
Electron Carrier concentration (n) using equation (4)
Potential (Φ_i) using Poisson's equation shown in (1)
$\frac{\Delta\Phi_i}{\Phi_i} < 0.001$
Yes
No
Good agreement with TB Method: Φ and n ?
Yes
No
Exit
Update m_{ox} , m_{st} and Energy Correction for Ground (ΔE_0) and other excited states (ΔE_1)
Update Potential

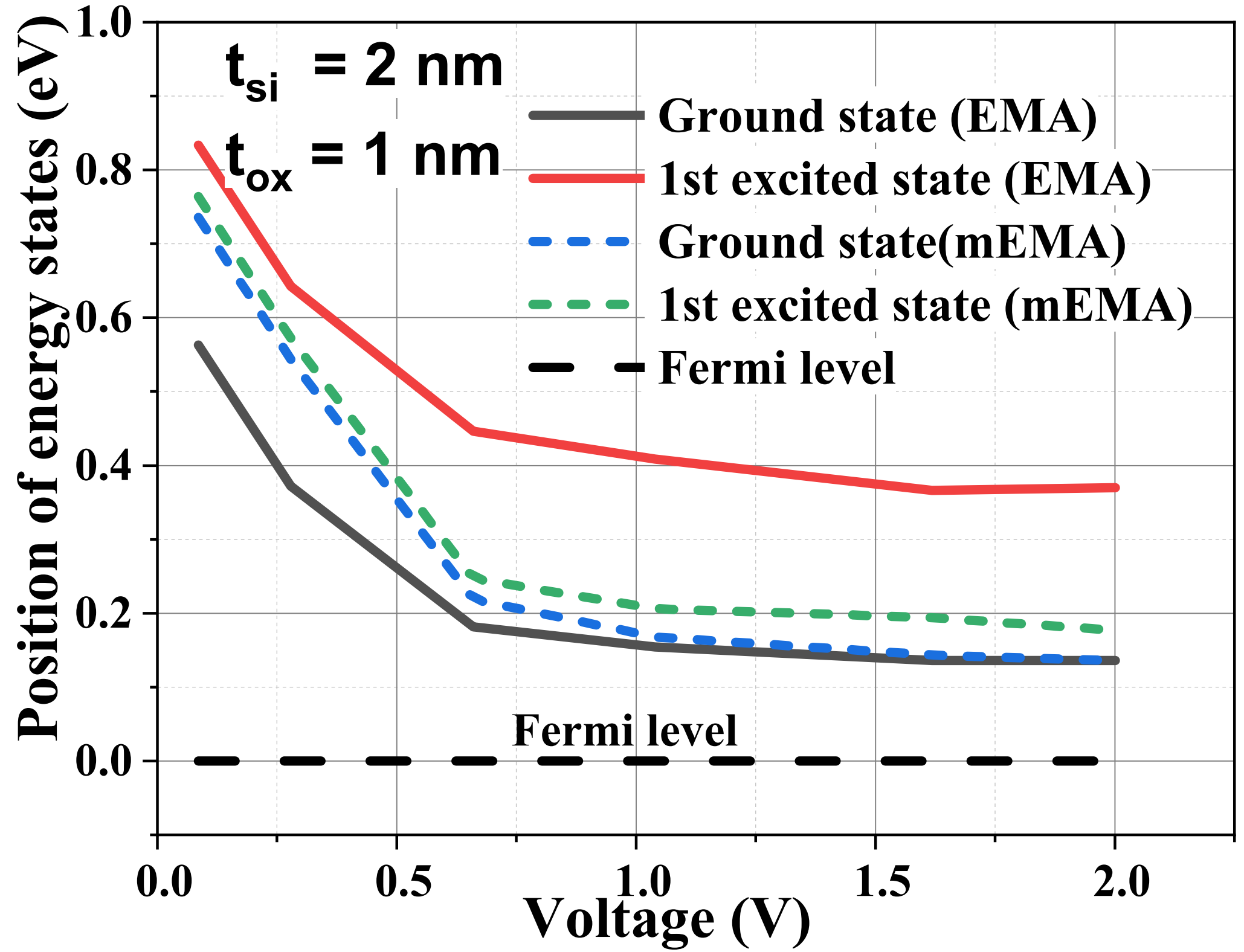
t_{si} = 2 nm
t_{ox} = 1 nm
Ground state (EMA)
1st excited state (EMA)
Ground state(mEMA)
1st excited state (mEMA)
Fermi level
Fermi level
Position of energy states (eV)
Voltage (V)
1.0
0.8
0.6
0.4
0.2
0.0
0.0
0.5
1.0
1.5
2.0

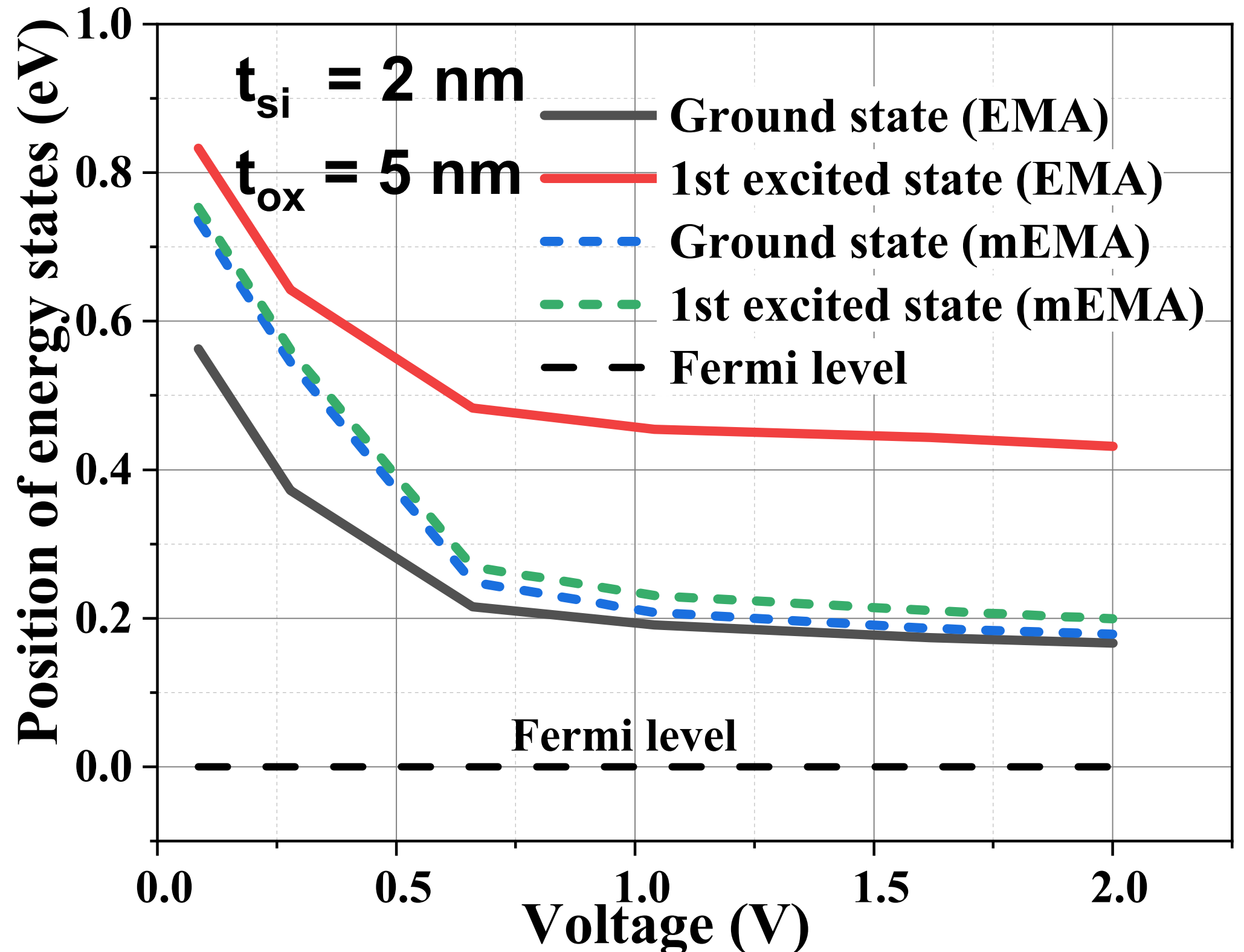
t_{si} = 2 nm
t_{ox} = 5 nm
Ground state (EMA)
1st excited state (EMA)
Ground state (mEMA)
1st excited state (mEMA)
Fermi level
Fermi level
Position of energy states (eV)
Voltage (V)
1.0
0.8
0.6
0.4
0.2
0.0
0.0
0.5
1.0
1.5
2.0

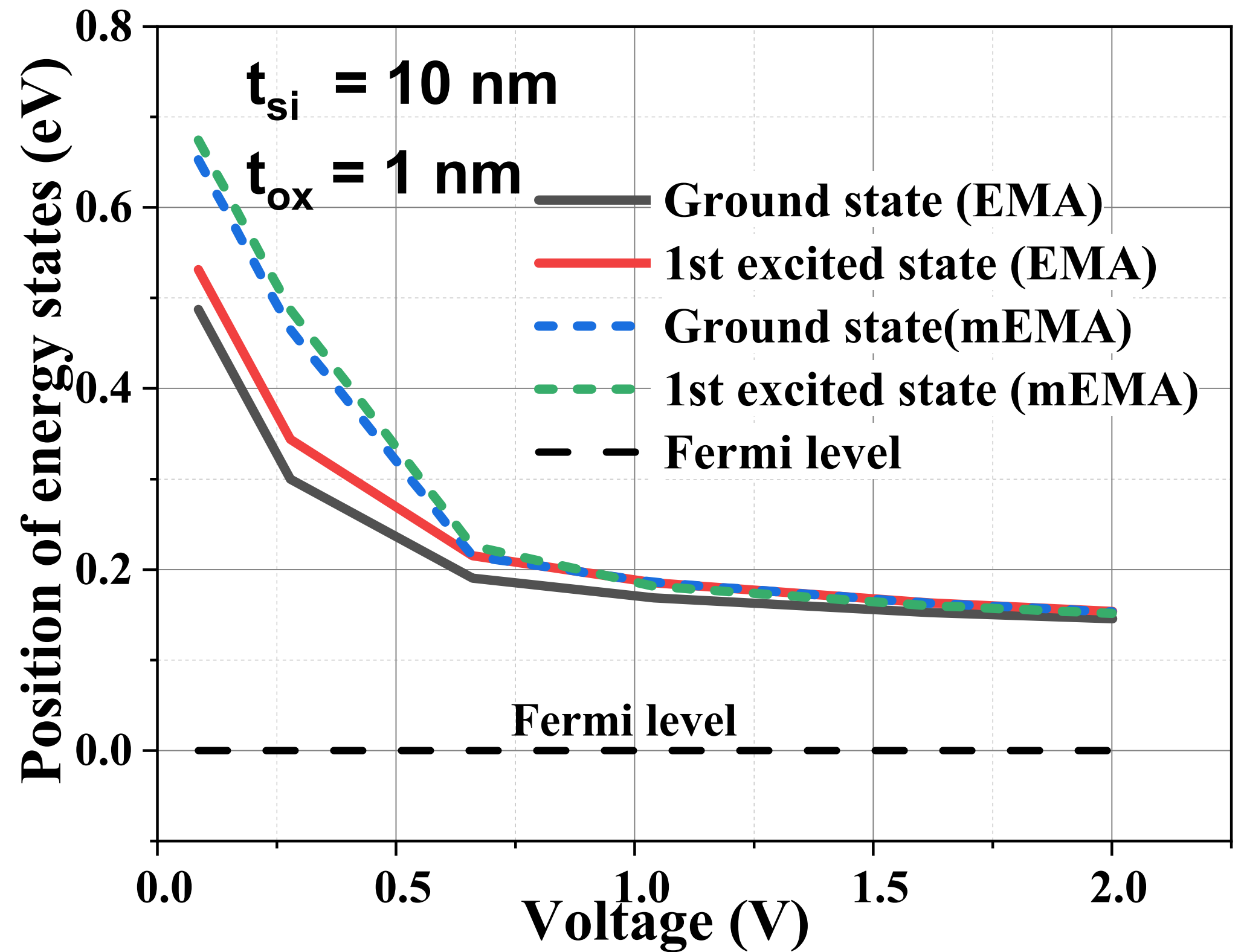
t_{si} = 10 nm
t_{ox} = 1 nm
Ground state (EMA)
1st excited state (EMA)
Ground state(mEMA)
1st excited state (mEMA)
Fermi level
Fermi level
Position of energy states (eV)
Voltage (V)
0.8
0.6
0.4
0.2
0.0
0.0
0.5
1.0
1.5
2.0

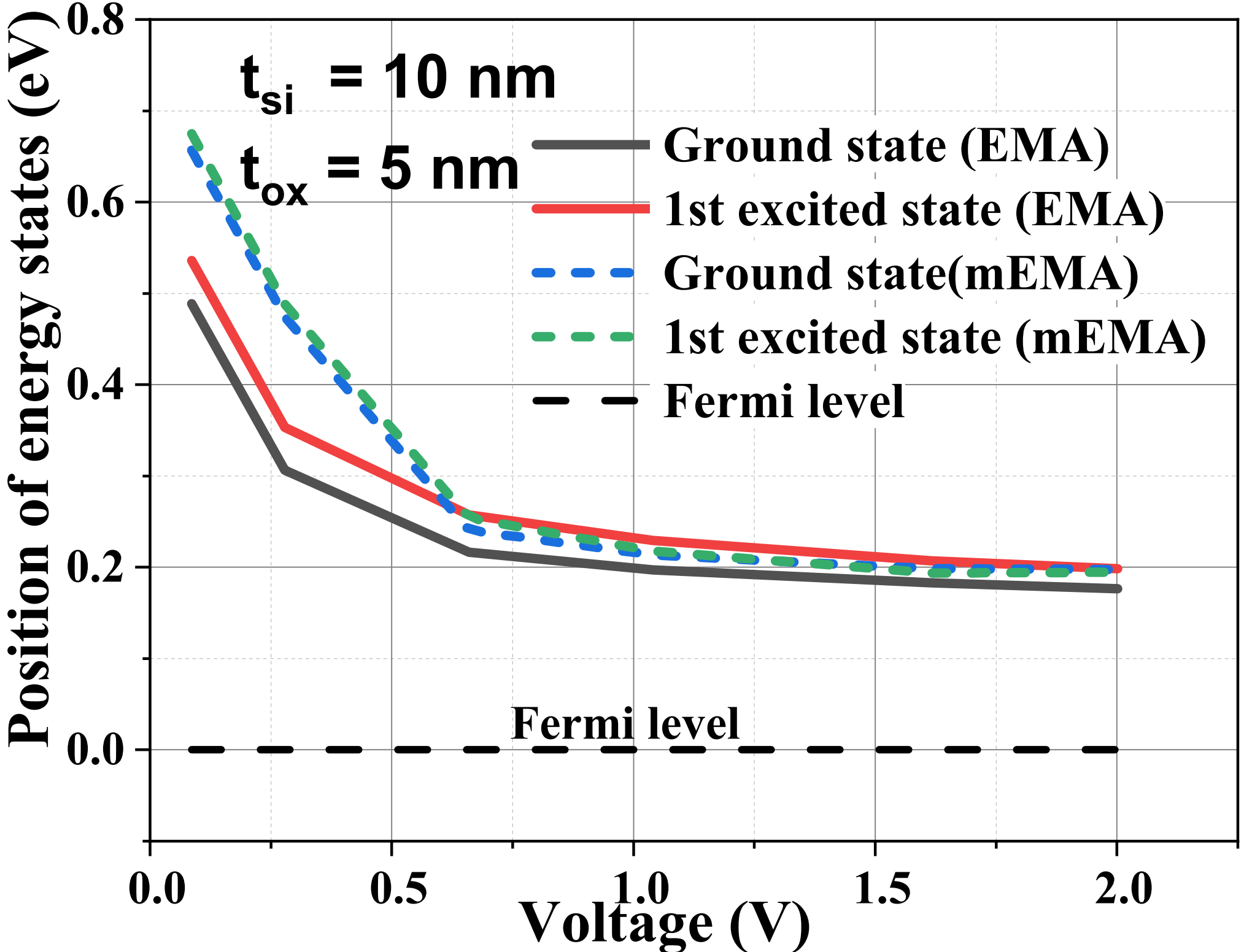
t_{si} = 10 nm
t_{ox} = 5 nm
Ground state (EMA)
1st excited state (EMA)
Ground state(mEMA)
1st excited state (mEMA)
Fermi level
Fermi level
Position of energy states (eV)
0.8
0.6
0.4
0.2
0.0
0.0
0.5
1.0
1.5
2.0
Voltage (V)

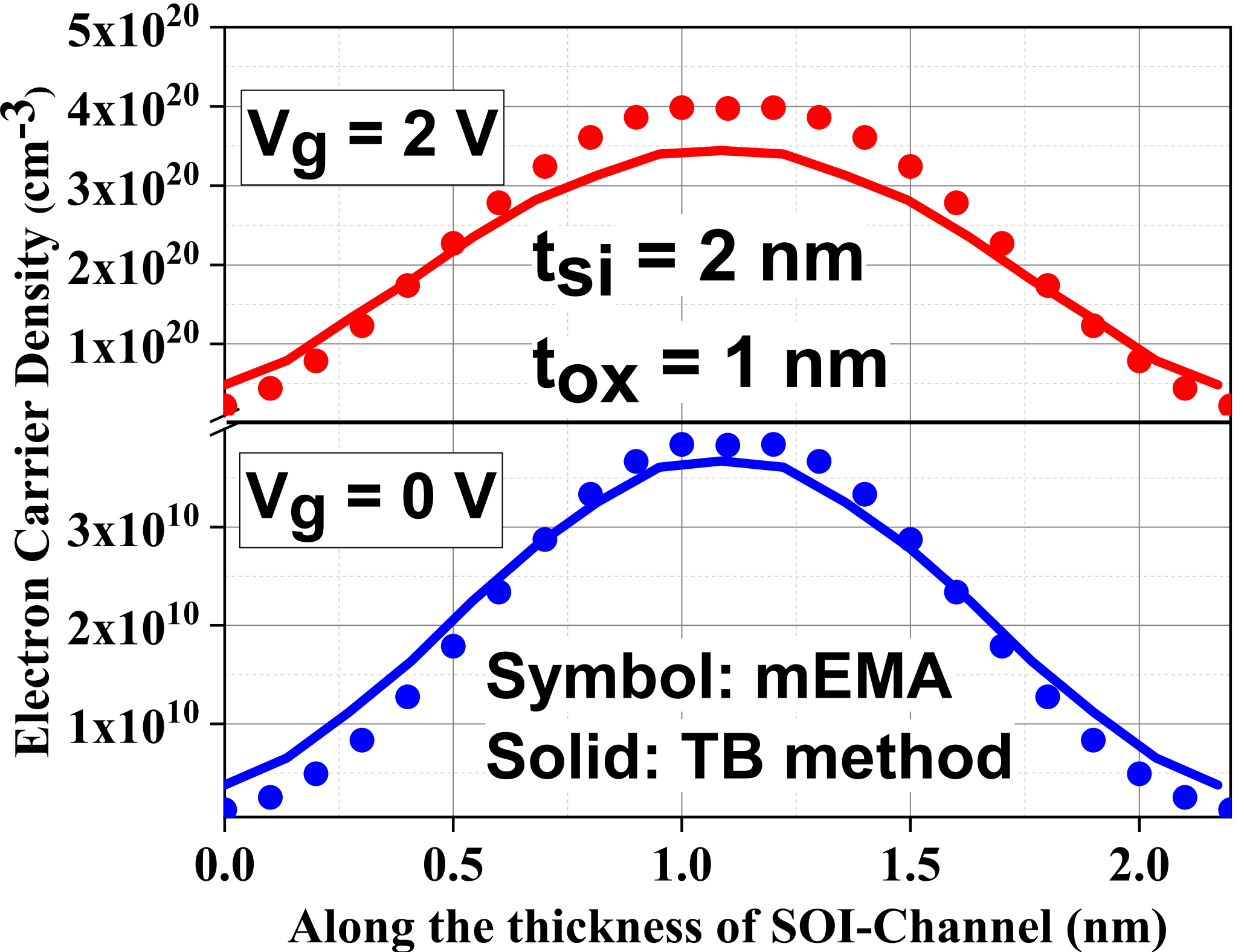
Electron Carrier Density (cm-3)
5x10^20
4x10^20
3x10^20
2x10^20
1x10^20
Vg = 2 V
tsi = 2 nm
tox = 1 nm
3x10^10
2x10^10
1x10^10
Vg = 0 V
Symbol: mEMA
Solid: TB method
0.0
0.5
1.0
1.5
2.0
Along the thickness of SOI-Channel (nm)

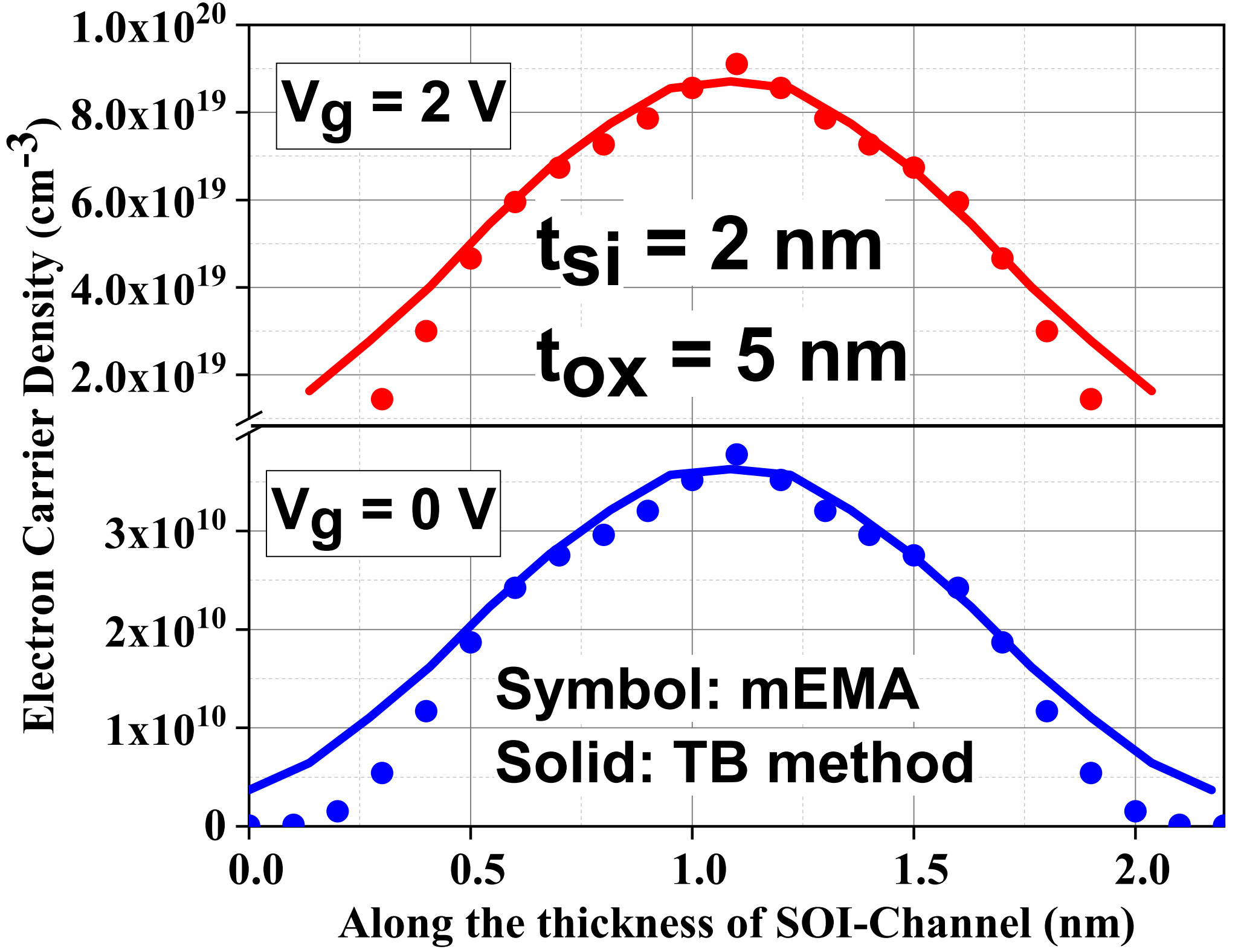
Vg = 2 V
tsi = 2 nm
tox = 5 nm
Vg = 0 V
Symbol: mEMA
Solid: TB method
Electron Carrier Density (cm-3)
Along the thickness of SOI-Channel (nm)
1.0x10^20
8.0x10^19
6.0x10^19
4.0x10^19
2.0x10^19
3x10^10
2x10^10
1x10^10
0
0.0
0.5
1.0
1.5
2.0

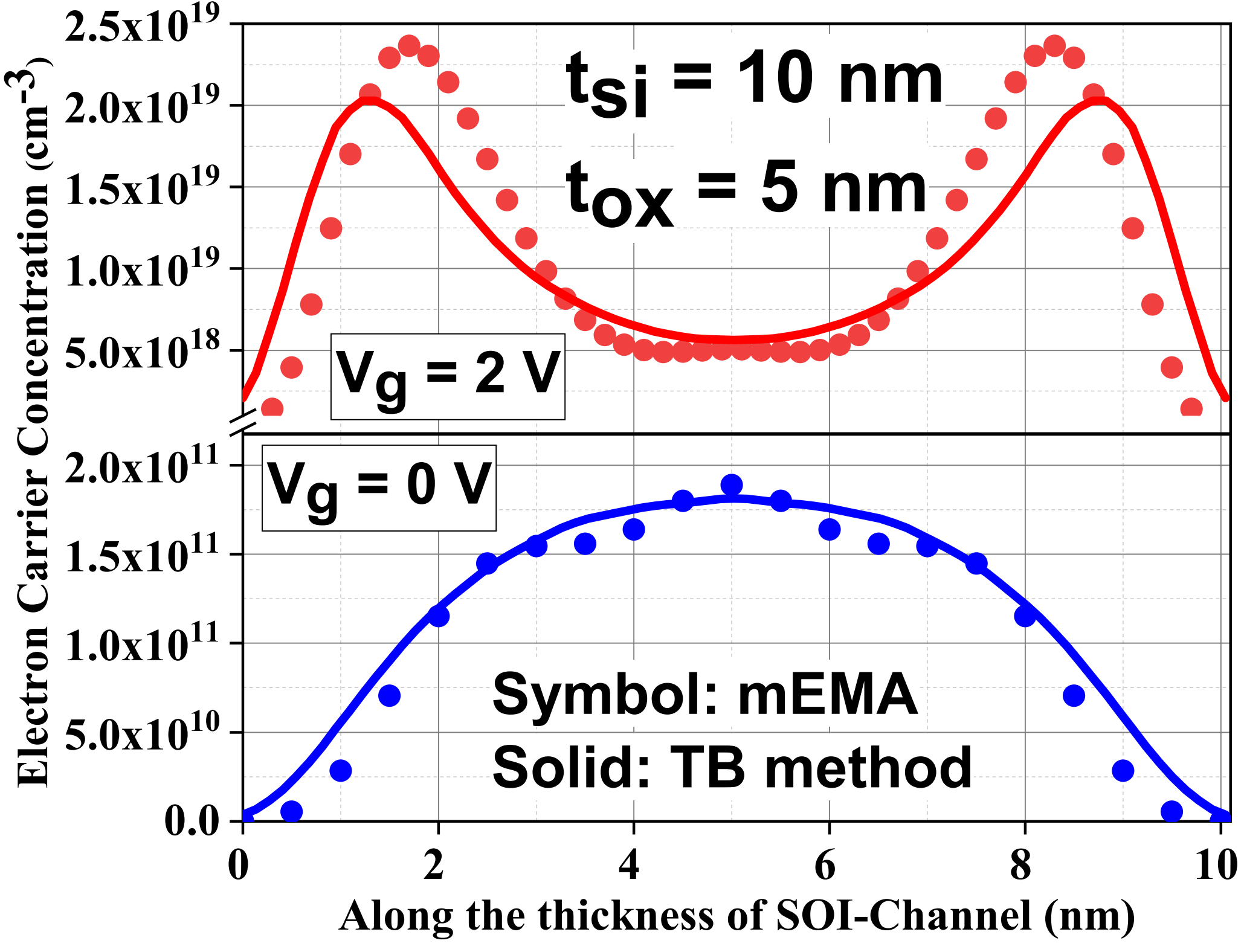
t_{si} = 10 nm
t_{ox} = 5 nm
V_g = 2 V
V_g = 0 V
Symbol: mEMA
Solid: TB method
Electron Carrier Concentration (cm^{-3})
2.5x10^{19}
2.0x10^{19}
1.5x10^{19}
1.0x10^{19}
5.0x10^{18}
2.0x10^{11}
1.5x10^{11}
1.0x10^{11}
5.0x10^{10}
0.0
0
2
4
6
8
10
Along the thickness of SOI-Channel (nm)

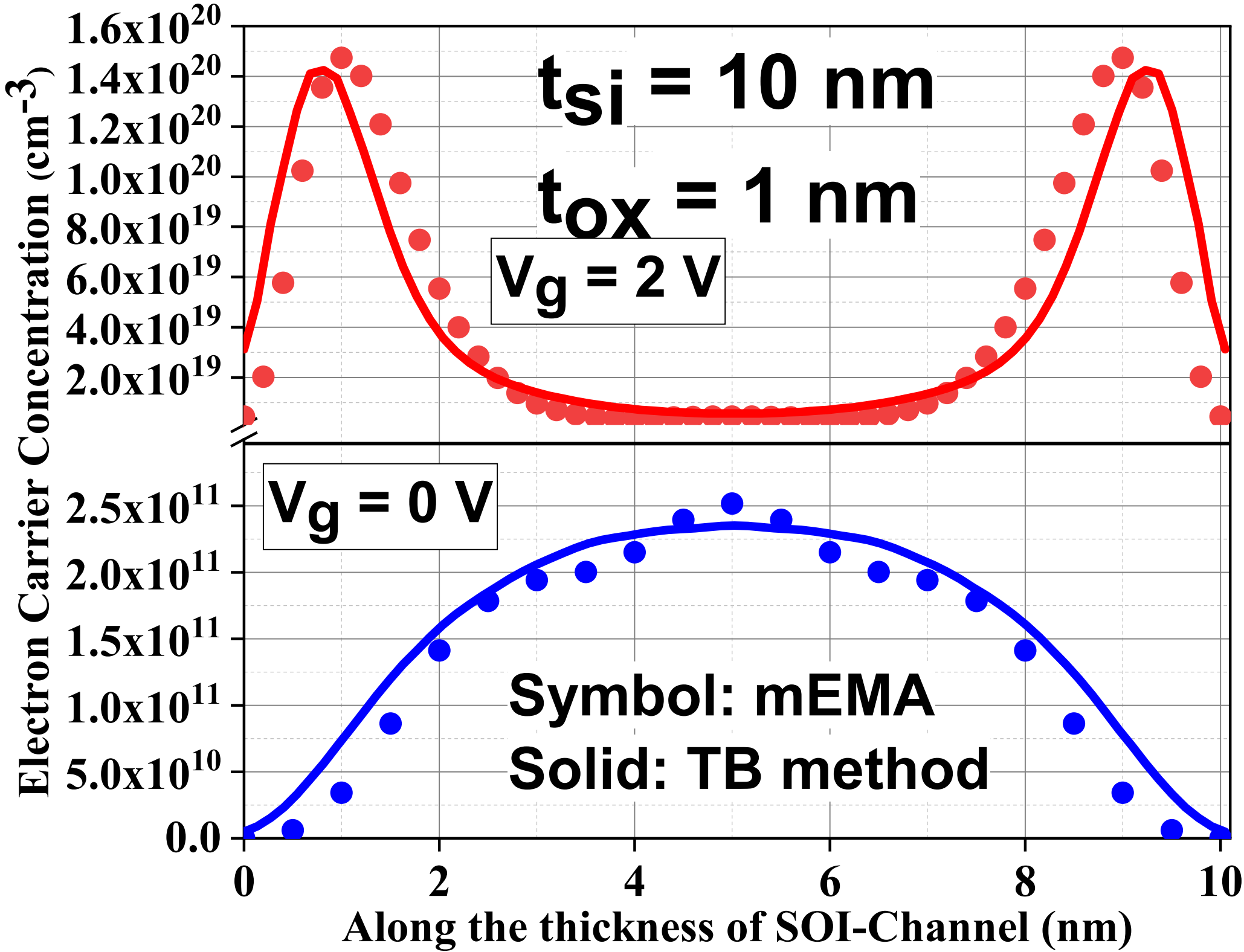
t_{si} = 10 nm
t_{ox} = 1 nm
V_g = 2 V
V_g = 0 V
Symbol: mEMA
Solid: TB method
Electron Carrier Concentration (cm^{-3})
1.6x10^20
1.4x10^20
1.2x10^20
1.0x10^20
8.0x10^19
6.0x10^19
4.0x10^19
2.0x10^19
2.5x10^11
2.0x10^11
1.5x10^11
1.0x10^11
5.0x10^10
0.0
0
2
4
6
8
10
Along the thickness of SOI-Channel (nm)

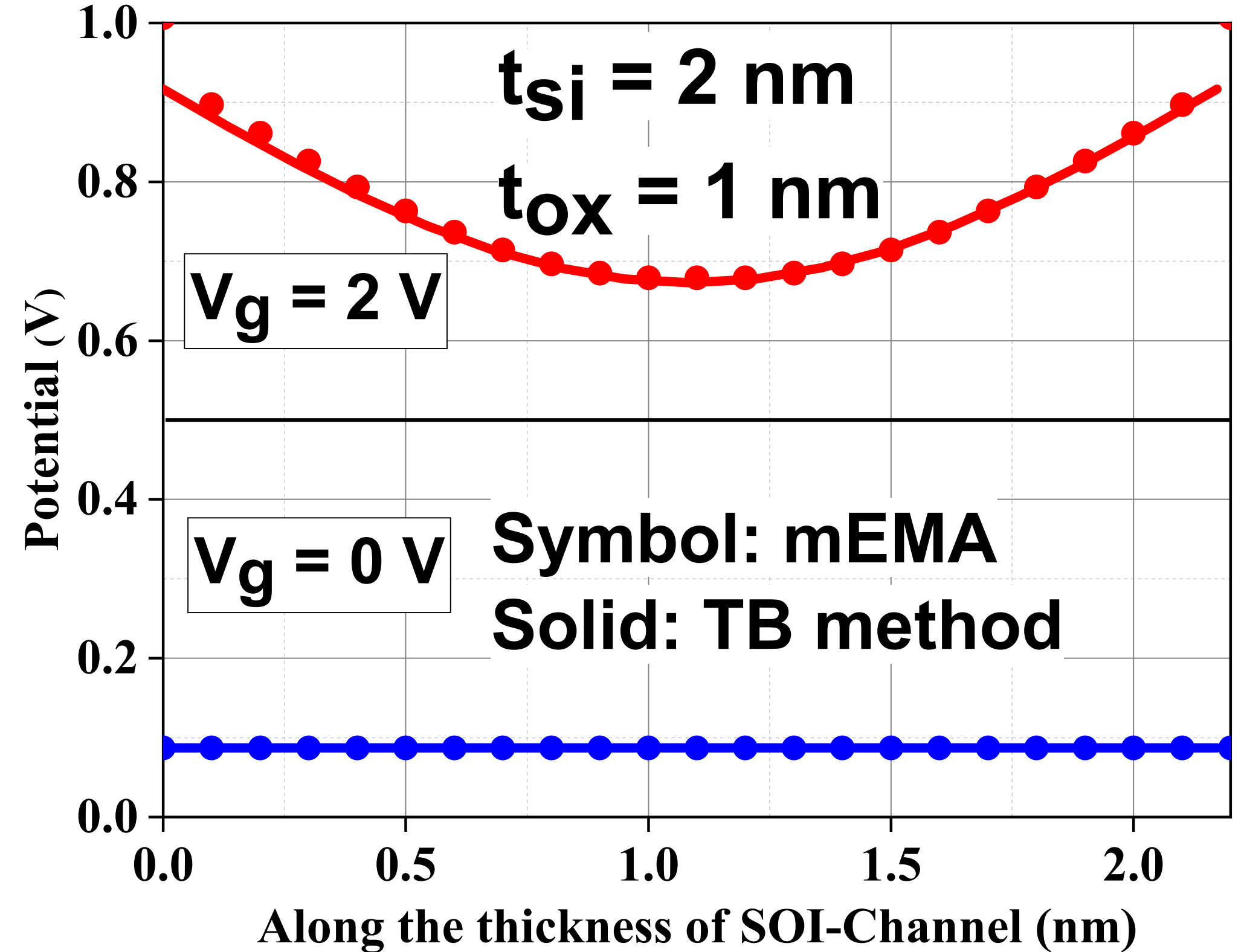
t_{si} = 2 nm
t_{ox} = 1 nm
V_g = 2 V
V_g = 0 V
Symbol: mEMA
Solid: TB method
Potential (V)
Along the thickness of SOI-Channel (nm)
1.0
0.8
0.6
0.4
0.2
0.0
0.0
0.5
1.0
1.5
2.0

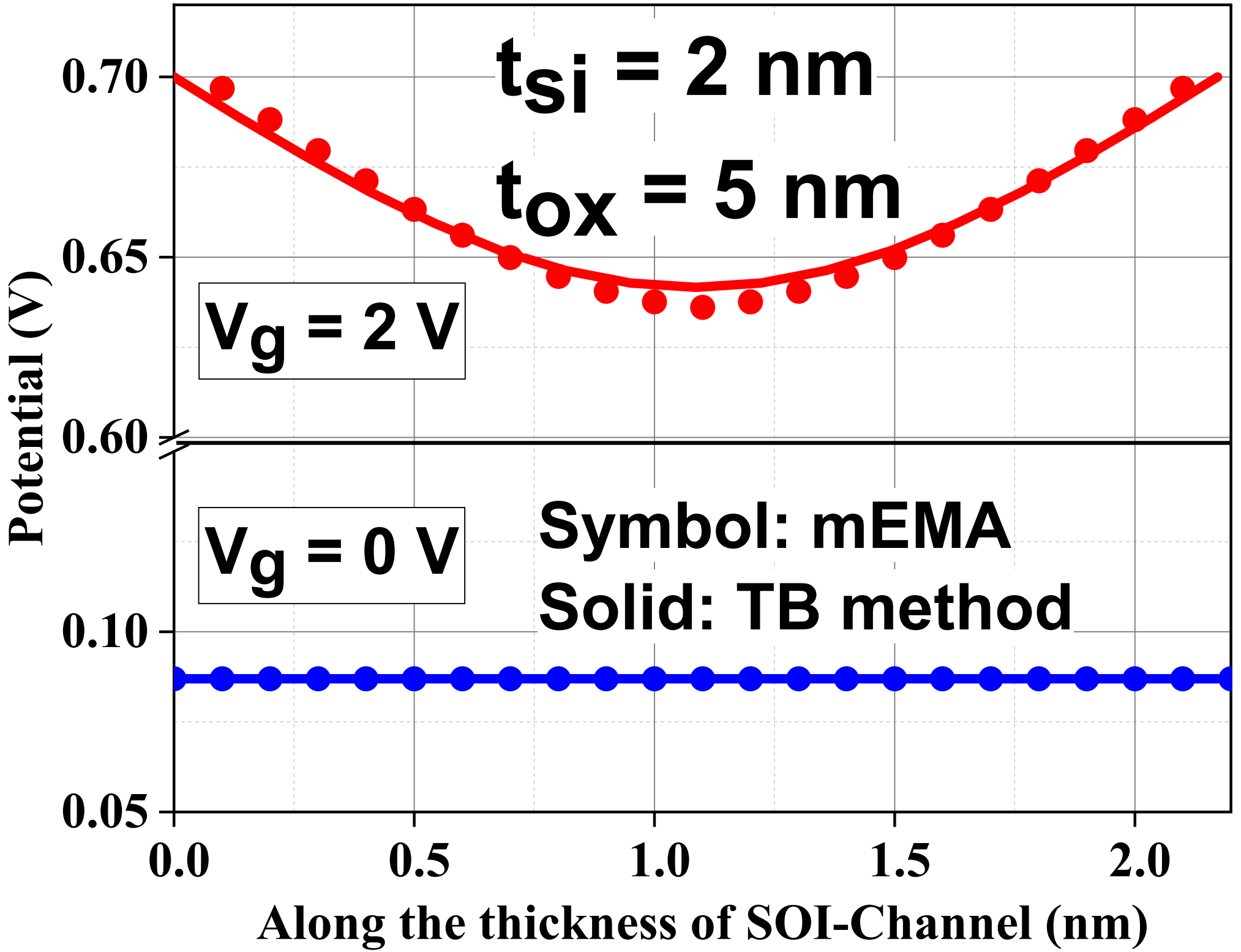
t_{si} = 2 nm
t_{ox} = 5 nm
V_g = 2 V
V_g = 0 V
Symbol: mEMA
Solid: TB method
Potential (V)
0.70
0.65
0.60
0.10
0.05
0.0
0.5
1.0
1.5
2.0
Along the thickness of SOI-Channel (nm)

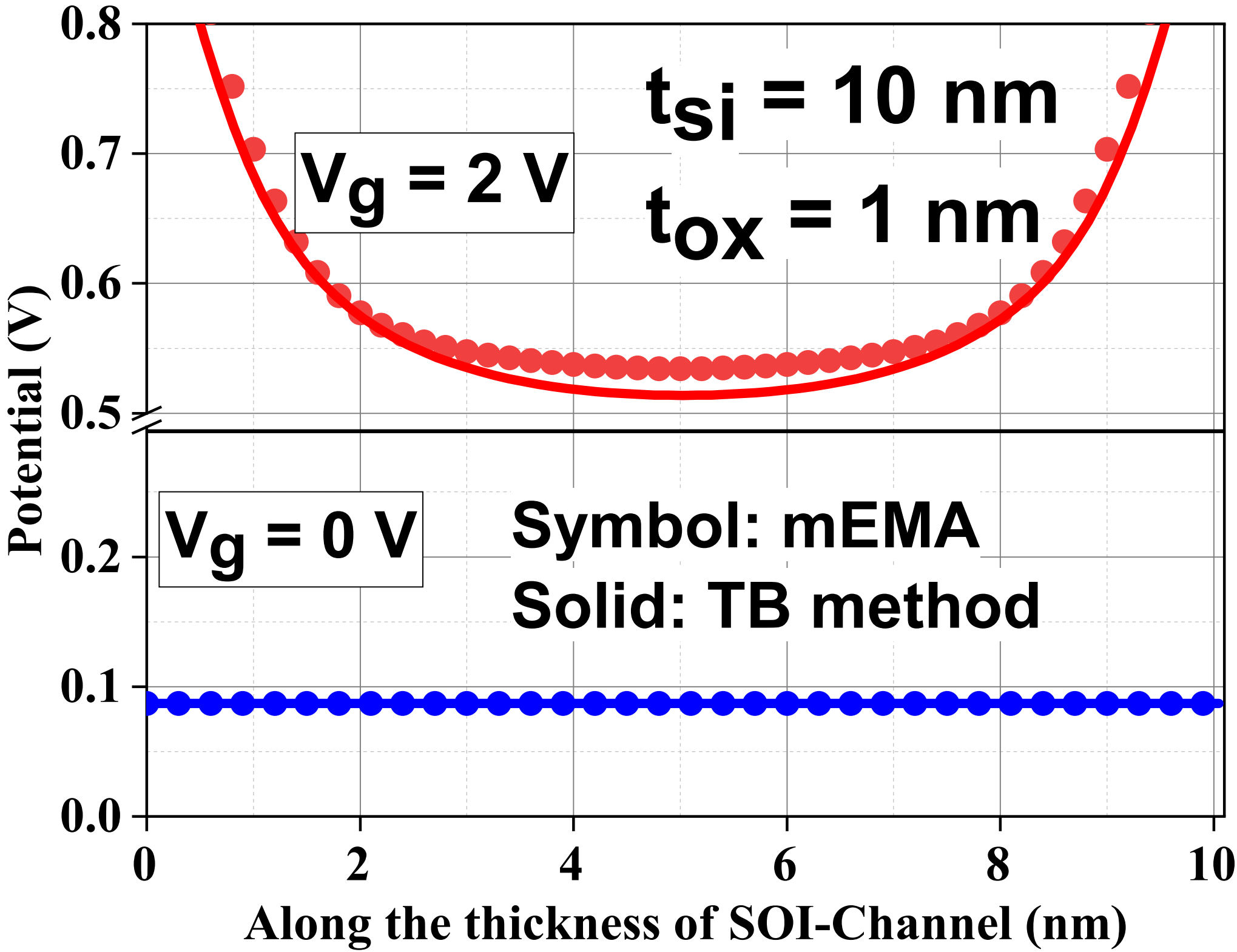
0.8
0.7
0.6
0.5
0.2
0.1
0.0
Potential (V)
V_g = 2 V
t_{si} = 10 nm
t_{ox} = 1 nm
V_g = 0 V
Symbol: mEMA
Solid: TB method
0
2
4
6
8
10
Along the thickness of SOI-Channel (nm)

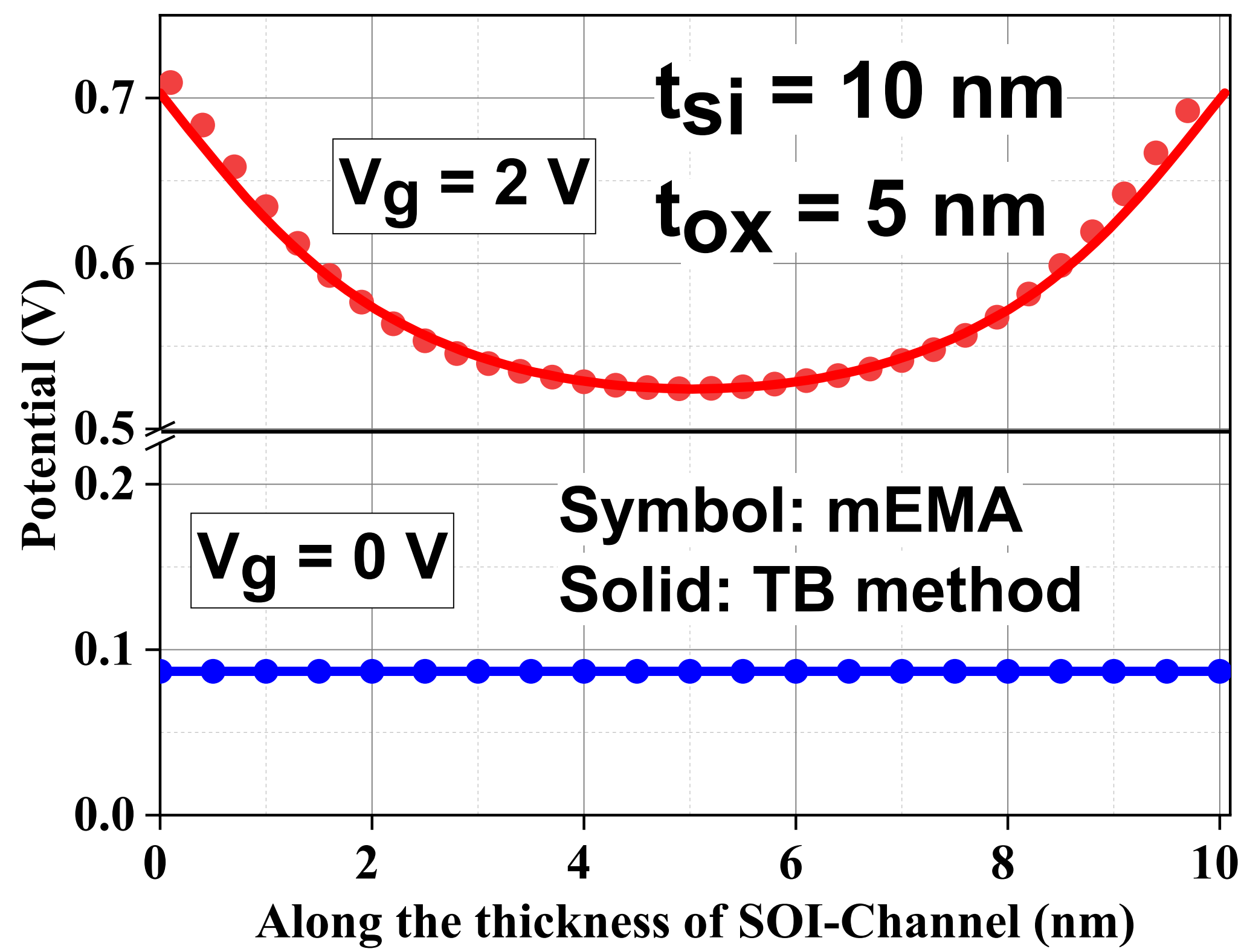
t_{si} = 10 nm
t_{ox} = 5 nm
V_g = 2 V
V_g = 0 V
Symbol: mEMA
Solid: TB method
Potential (V)
Along the thickness of SOI-Channel (nm)
0.7
0.6
0.5
0.2
0.1
0.0
0
2
4
6
8
10

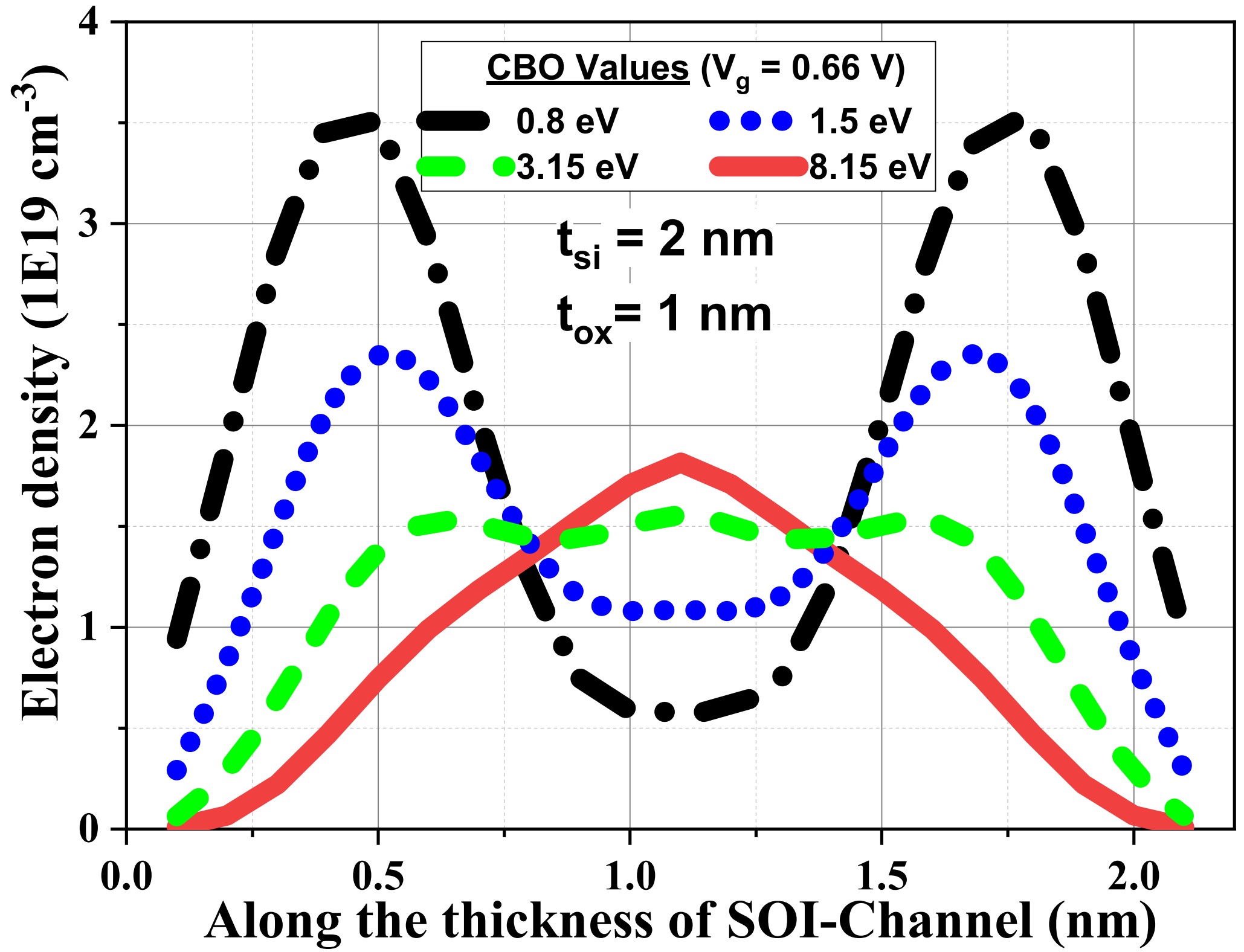
CBO Values (V_g = 0.66 V)
0.8 eV
1.5 eV
3.15 eV
8.15 eV
t_si = 2 nm
t_ox = 1 nm
Electron density (1E19 cm^-3)
Along the thickness of SOI-Channel (nm)
0
1
2
3
4
0.0
0.5
1.0
1.5
2.0

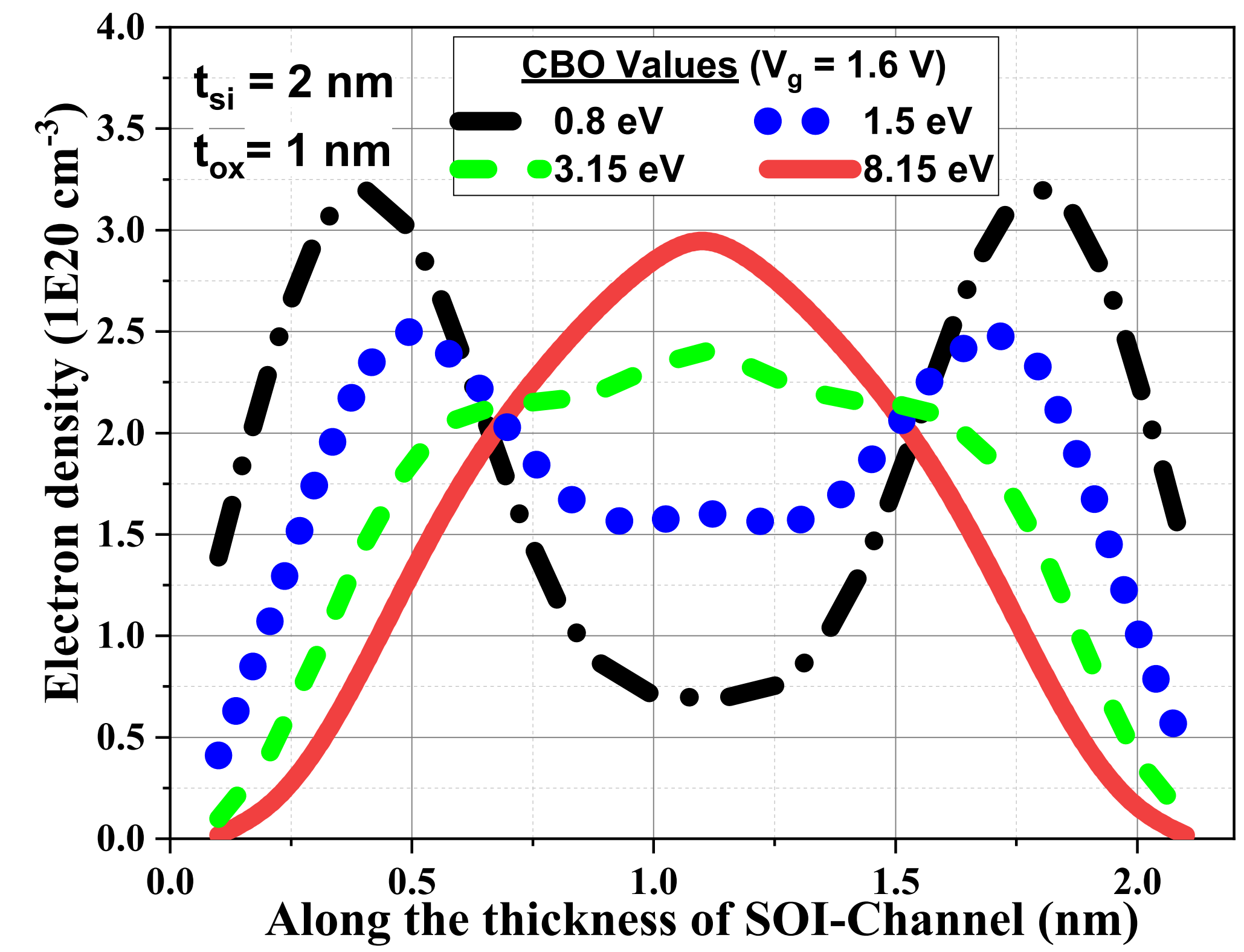
t_{si} = 2 nm
t_{ox}= 1 nm
CBO Values (V_g = 1.6 V)
0.8 eV
1.5 eV
3.15 eV
8.15 eV
Electron density (1E20 cm^{-3})
Along the thickness of SOI-Channel (nm)
0.0
0.5
1.0
1.5
2.0
2.5
3.0
3.5
4.0

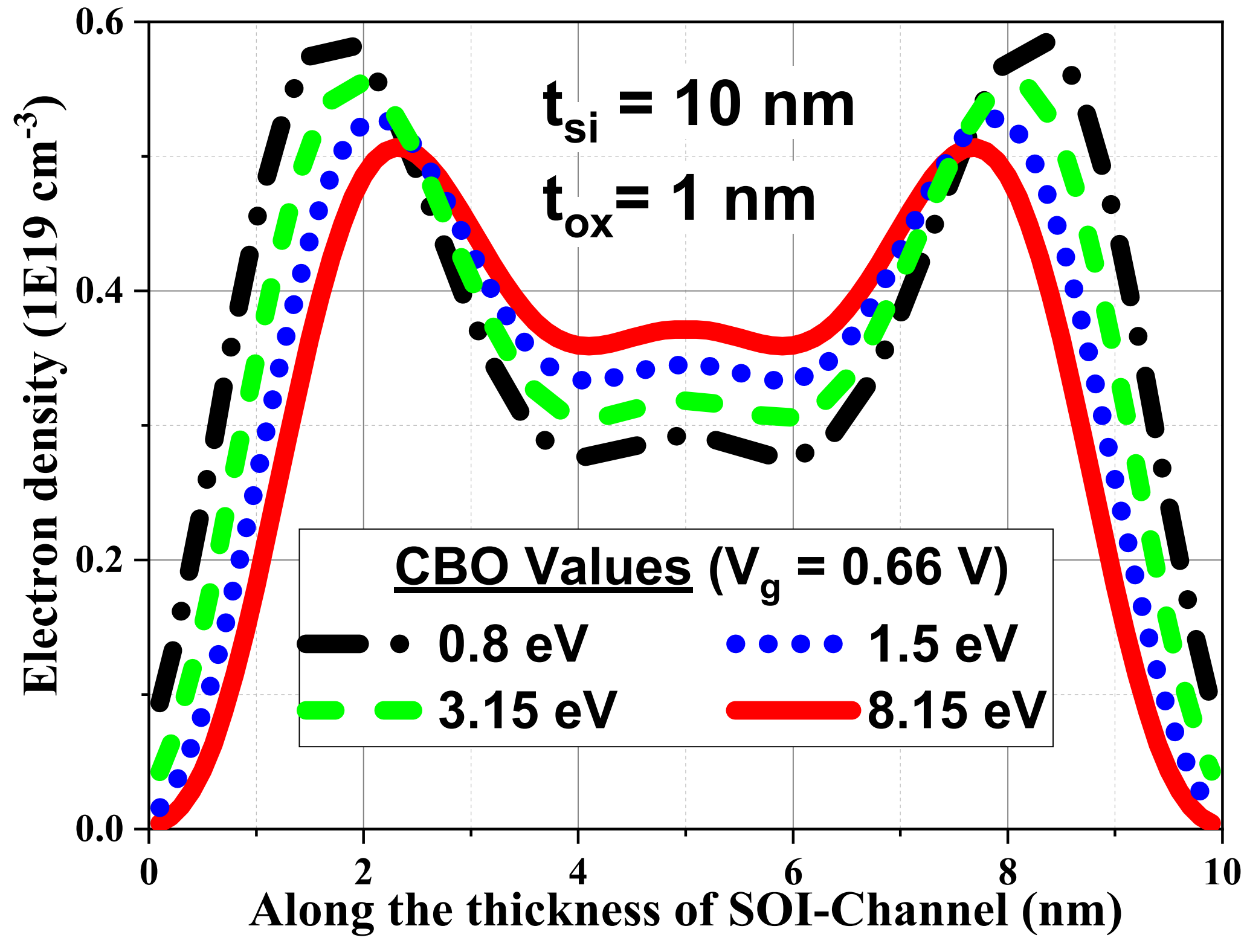
0.6
0.4
0.2
0.0
Electron density (1E19 cm-3)
tsi = 10 nm
tox = 1 nm
CBO Values (Vg = 0.66 V)
0.8 eV
1.5 eV
3.15 eV
8.15 eV
0
2
4
6
8
10
Along the thickness of SOI-Channel (nm)

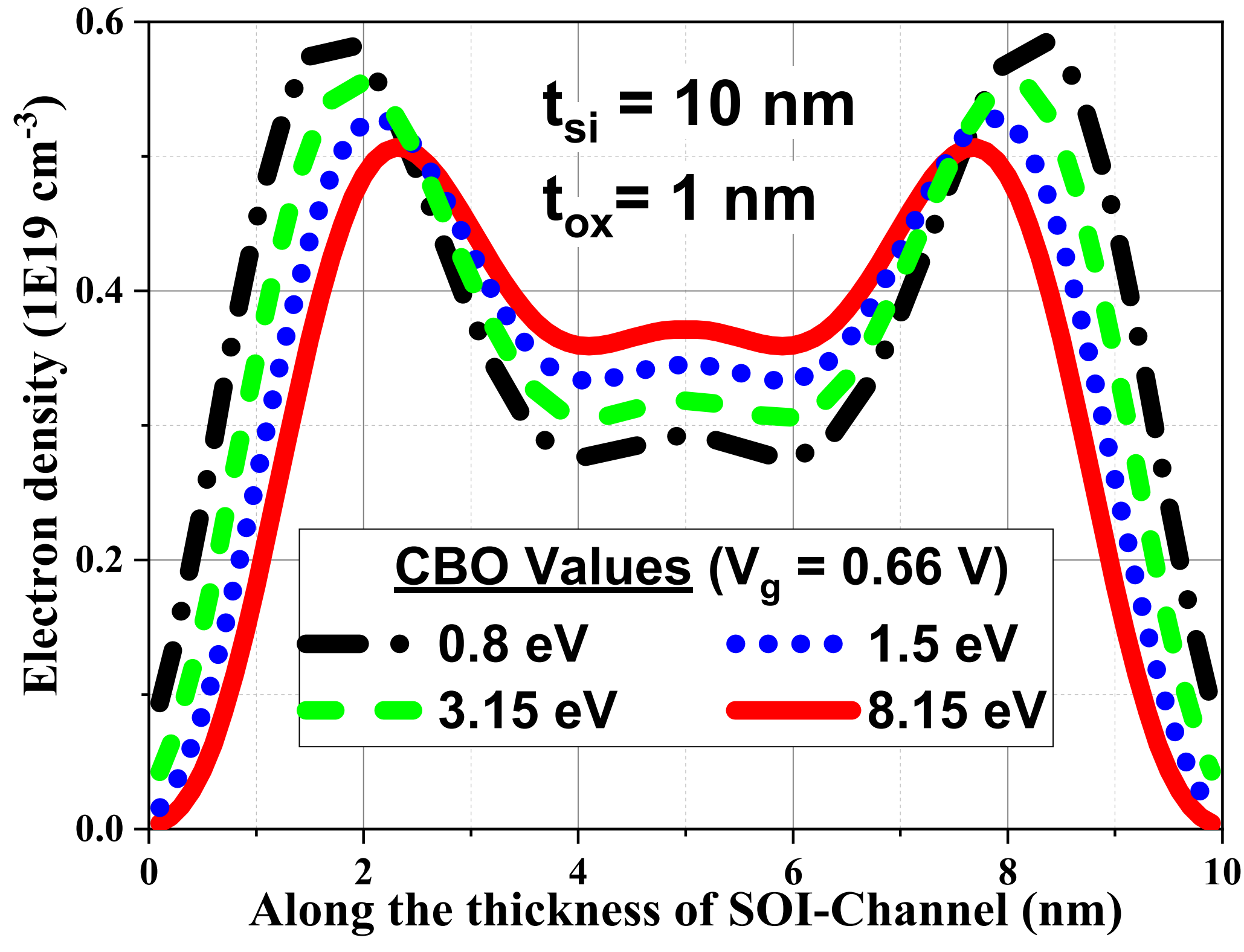
0.6
0.4
0.2
0.0
Electron density (1E19 cm-3)
tsi = 10 nm
tox = 1 nm
CBO Values (Vg = 0.66 V)
0.8 eV
1.5 eV
3.15 eV
8.15 eV
0
2
4
6
8
10
Along the thickness of SOI-Channel (nm)

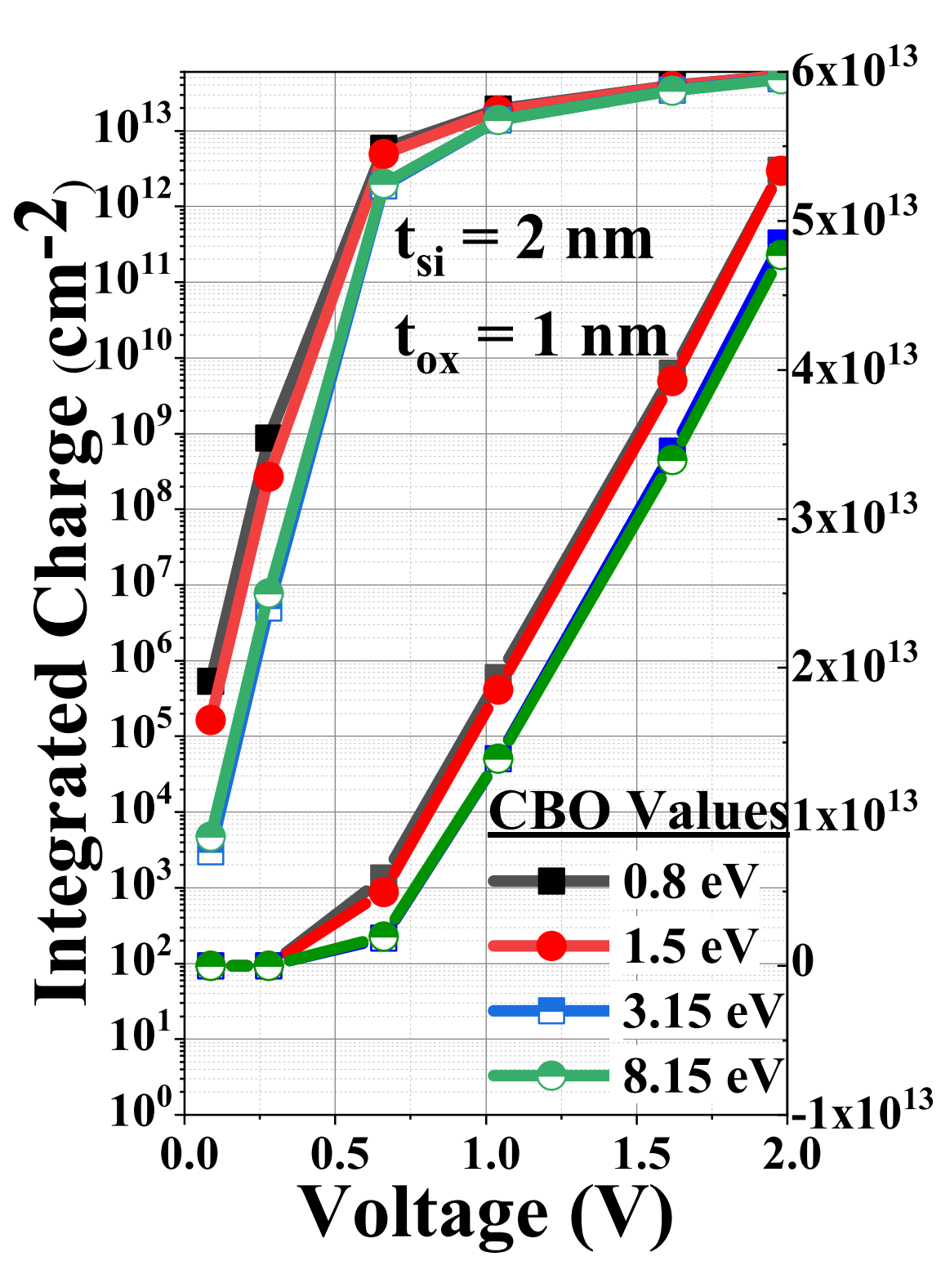
Integrated Charge (cm-2)
Voltage (V)
tsi = 2 nm
tox = 1 nm
CBO Values
0.8 eV
1.5 eV
3.15 eV
8.15 eV
10^13
10^12
10^11
10^10
10^9
10^8
10^7
10^6
10^5
10^4
10^3
10^2
10^1
10^0
6x10^13
5x10^13
4x10^13
3x10^13
2x10^13
1x10^13
0
-1x10^13
0.0
0.5
1.0
1.5
2.0

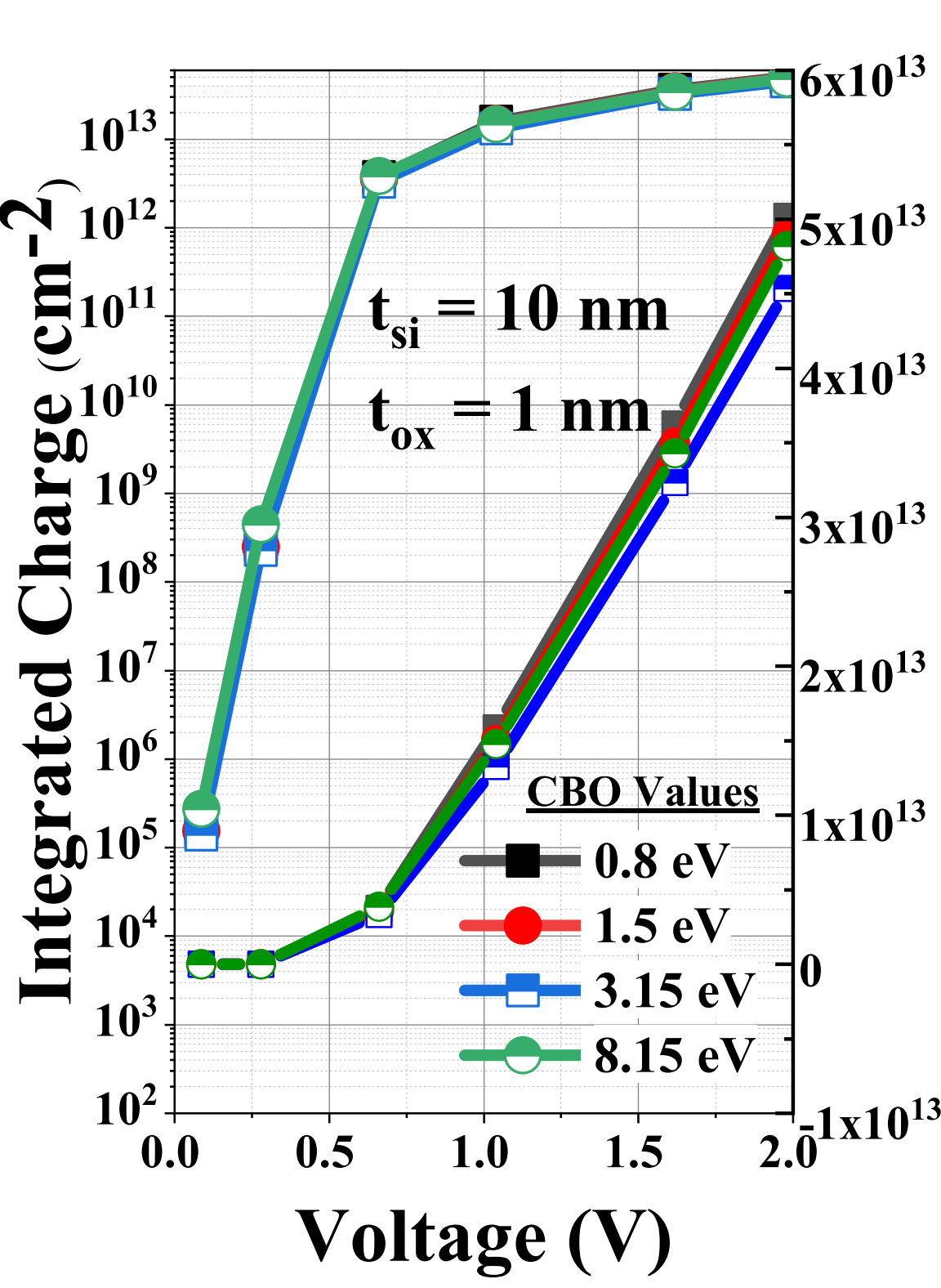
Integrated Charge (cm-2)
Voltage (V)
tsi = 10 nm
tox = 1 nm
CBO Values
0.8 eV
1.5 eV
3.15 eV
8.15 eV
10^13
10^12
10^11
10^10
10^9
10^8
10^7
10^6
10^5
10^4
10^3
10^2
6x10^13
5x10^13
4x10^13
3x10^13
2x10^13
1x10^13
0
-1x10^13
0.0
0.5
1.0
1.5
2.0

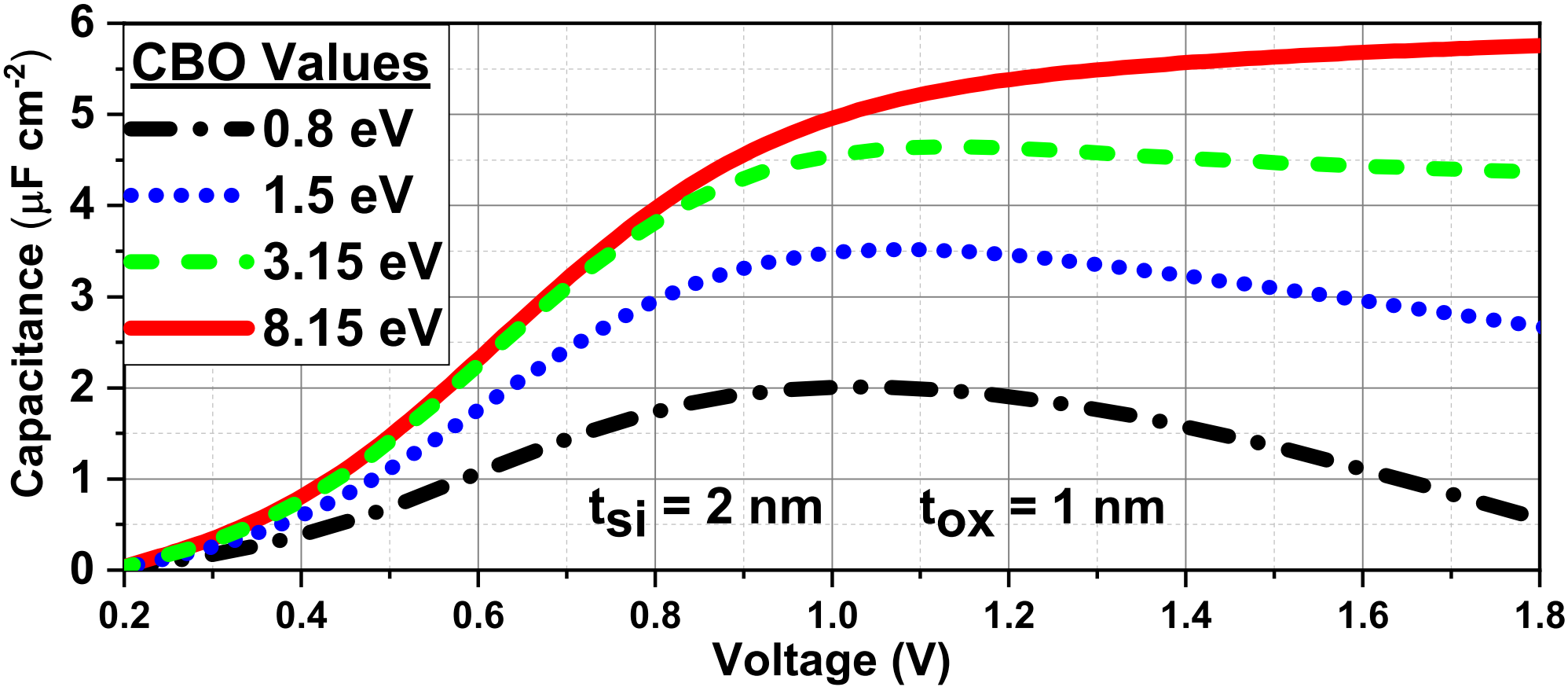
CBO Values
0.8 eV
1.5 eV
3.15 eV
8.15 eV
t_{si} = 2 nm
t_{ox} = 1 nm
Capacitance (μF cm^{-2})
Voltage (V)
0
1
2
3
4
5
6
0.2
0.4
0.6
0.8
1.0
1.2
1.4
1.6
1.8

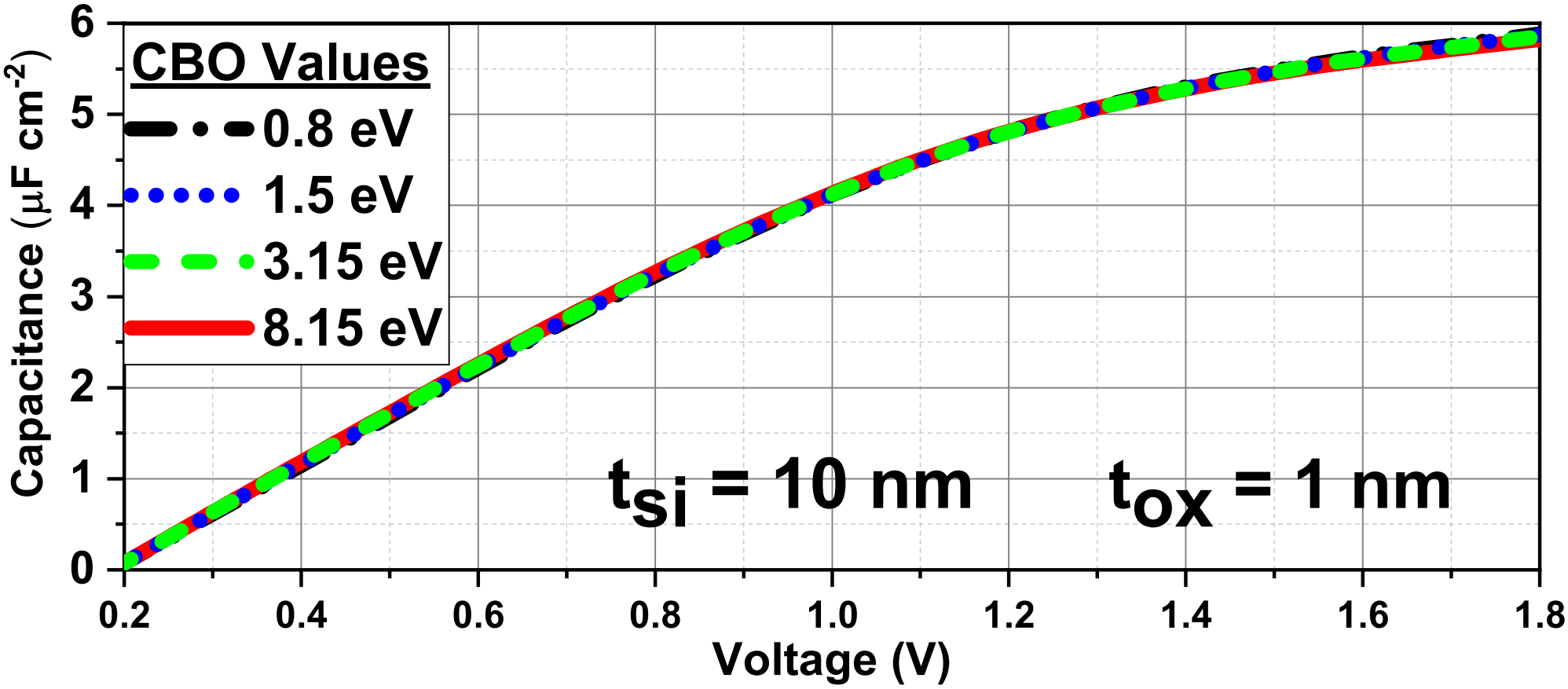
CBO Values
0.8 eV
1.5 eV
3.15 eV
8.15 eV
t_{si} = 10 nm
t_{ox} = 1 nm
Capacitance (μF cm^{-2})
Voltage (V)
0
1
2
3
4
5
6
0.2
0.4
0.6
0.8
1.0
1.2
1.4
1.6
1.8